



GB04/1851



INVESTOR IN PEOPLE

The Patent Office
Concept House
Cardiff Road
Newport
South Wales
NP10 8QQ

REC'D 19 APR 2004

WIPO

PCT

I, the undersigned, being an officer duly authorised in accordance with Section 74(1) and (4) of the Deregulation & Contracting Out Act 1994, to sign and issue certificates on behalf of the Comptroller-General, hereby certify that annexed hereto is a true copy of the documents as originally filed in connection with the patent application identified therein.

In accordance with the Patents (Companies Re-registration) Rules 1982, if a company named in this certificate and any accompanying documents has re-registered under the Companies Act 1980 with the same name as that with which it was registered immediately before re-registration save for the substitution as, or inclusion as, the last part of the name of the words "public limited company" or their equivalents in Welsh, references to the name of the company in this certificate and any accompanying documents shall be treated as references to the name with which it is so re-registered.

In accordance with the rules, the words "public limited company" may be replaced by p.l.c., plc, P.L.C. or PLC.

Re-registration under the Companies Act does not constitute a new legal entity but merely subjects the company to certain additional company law rules.

Best Available Copy

Signed

Andrew

Dated

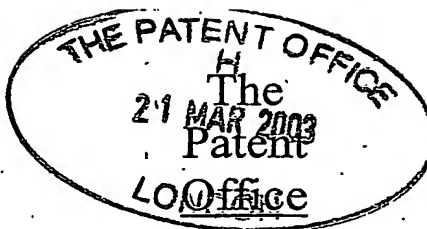
8 April 2004

**PRIORITY
DOCUMENT**

SUBMITTED OR TRANSMITTED IN
COMPLIANCE WITH RULE 17.1(a) OR (b)

Patents Form 1/77

Patents Act 1977
(Rule 16)



1/77

24MAR03 E794384-1 000001
P01/7700 0.00-0306606.5

Request for grant of a patent

The Patent Office
Cardiff Road
Newport
Gwent NP9 1RH

| | | | | |
|----|--|---|--|------------------------------------|
| 1. | Your reference | MPC/9379 GB | | |
| 2. | Patent application number (The Patent Office will fill in this part) | 0306606.5 | | 21 MAR 2003 |
| 3. | Full name, address and postcode of the or of each applicant (underline all surnames) | BlazePhotonics Limited Finance office, University of Bath The Avenue, Claverton Down Bath BA2 7AY United Kingdom | | |
| | Patents ADP number (if you know it) | 814129001 | | |
| | If the applicant is a corporate body, give the country/state of its incorporation | United Kingdom | | |
| 4. | Title of the invention | Improvements in and relating to optical waveguides. | | |
| 5. | Name of your agent (if you have one) | Abel & Imray | | |
| | "Address for service" in the United Kingdom to which all correspondence should be sent (including the postcode) | 20 Red Lion Street London WC1R 4PQ | | |
| | Patents ADP number (if you know it) | 174001 ✓ | | |
| 6. | If you are declaring priority from one or more earlier patent applications, give the country and the date of filing of the or of each of these earlier applications and (if you know it) the or each application number | Country | Priority application number (if you know it) | Date of filing (day/month/year) |
| 7. | If this application is divided or otherwise derived from an earlier UK application, give the number and the filing date of the earlier application | Number of earlier application | Date of filing (day/month/year) | |
| 8. | Is a statement of inventorship and of right to grant of a patent required in support of this request? (Answer 'Yes' if: a) any applicant named in part 3 is not an inventor, or b) there is an inventor who is not named as an applicant, or c) any named applicant is a corporate body. See note (d)) | Yes | | |

9. Enter the number of sheets for any of the following items you are filing with this form.

Do not count copies of the same documents.

Continuation sheets of this form

Description 36 /

Claim(s) 8 /

Abstract

Drawing(s) 17 + 17 *figs*

10. If you are also filing any of the following, state how many against each item.

Priority documents

Translations of priority documents

Statement of inventorship and right to grant of a patent (*Patents Form 7/77*)

Request for preliminary examination and search (*Patents Form 9/77*) 1 /

Request for substantive examination (*Patents Form 10/77*)

Any other documents
(*please specify*)

11.

I/We request the grant of a patent on the basis of this application.

Signature

Date

Abel & Imray

Abel & Imray

21 March 2003

12. Name and daytime telephone number of person to contact in the United Kingdom

Matthew Critten

(01225) 469914

Improvements in and relating to optical waveguides

This present invention is in the field of optical waveguides and relates in particular to optical waveguides that guide light by virtue of a photonic bandgap.

Optical fibre waveguides, which are able to guide light by virtue of a so-called photonic bandgap (PBG), were first proposed in 1995.

In, for example, "Full 2-D photonic bandgaps in silica/air structures", Birks et al., Electronics Letters, 26 October 1995, Vol. 31, No. 22, pp.1941-1942, it was proposed that a PBG may be created in an optical fibre by providing a dielectric cladding structure, which has a refractive index that varies periodically between high and low index regions, and a core defect in the cladding structure in the form of a hollow core. In the proposed cladding structure, periodicity was provided by an array of air holes that extended through a silica glass matrix material to provide a PBG structure through which certain wavelengths of light could not pass. It was proposed that light coupled into the hollow core defect would be unable to escape into the cladding due to the PBG and, thus, the light would remain localised in the core defect.

It was appreciated that light travelling through a hollow core defect, for example filled with air or even under vacuum, would suffer significantly less from undesirable effects, such as non-linearity and loss, compared with light travelling through a solid silica or doped silica fibre core. As such, it was appreciated that a PBG fibre may find application as a transmission fibre to transmit light over extremely long distances, for example across the Atlantic Ocean, without undergoing signal regeneration or as a high optical power delivery waveguide. In contrast, for standard index-guiding,

single mode optical fibre, signal regeneration is typically required approximately every 80 kilometres.

The first PBG fibres that were attempted by the inventors had a periodic cladding structure formed by a triangular lattice of circular air holes embedded in a solid silica matrix and surrounding a central air core defect. Such fibres were formed by stacking circular or hexagonal capillary tubes, incorporating a core defect into the cladding by omitting a central capillary of the stack, and then heating and drawing the stack, in a one or two step process, to form a fibre having the required structure. The first fibres made by this process had a core defect formed by the omission of a single capillary from the centre of the cladding structure.

International patent application PCT/GB00/01249 (The Secretary of State for Defence, UK), filed on 21 March 2000, proposed the first PBG fibre to have a so-called seven-cell core defect, surrounded by a cladding comprising a triangular lattice of air holes embedded in an all-silica matrix. The core defect was formed by omitting an inner capillary and, in addition, the six capillaries surrounding the inner capillary. This fibre structure was seen to guide one or two modes in the core defect, in contrast to the previous, single-cell core defect fibre, which appeared not to support any guided modes in the core defect.

According to PCT/GB00/01249, it appeared that the single-cell core defect fibre, by analogy to the density-of-states calculations in solid-state physics, would only support approximately 0.23 modes. That is, it was not surprising that the single-cell core defect fibre appeared to support no guided modes in its core defect. In contrast, based on the seven-fold increase in core defect area (increasing the core defect radius by a factor of $\sqrt{7}$), the seven-cell core defect fibre was predicted to support approximately 1.61 spatial modes in the core defect. This prediction was consistent with

the finding that the seven-cell core defect fibre did indeed appear to support at least one guided mode in its core defect.

A preferred fibre in PCT/GB00/01249 was described as having a core defect diameter of around $15\mu\text{m}$ and an air-filling fraction (AFF) - that is, the proportion by volume of air in the cladding - of greater than 15% and, preferably, greater than 30%.

In "Analysis of air-guiding photonic bandgap fibres", Optics Letters, Vol. 25, No. 2, January 15, 2000, Broeng et al. provided a theoretical analysis of PBG fibres. For a fibre with a seven-cell core defect and a cladding comprising a triangular lattice of near-circular holes, providing an AFF of around 70%, the structure was shown to support one or two air guided modes in the core defect. This was in line with the finding in PCT/GB00/01249.

In the chapter entitled "Photonic Crystal Fibers: Effective Index and Band-Gap Guidance" from the book "Photonic Crystal and Light Localization in the 21st Century", C.M. Soukoulis (ed.), ©2001 Kluwer Academic Publishers, the authors presented further analysis of PBG fibres based primarily on a seven-cell core defect fibre. The optical fibre was fabricated by stacking and drawing hexagonal silica capillary tubes. The authors suggested that a core defect must be large enough to support at least one guided mode but that, as in conventional fibres, increasing the core defect size would lead to the appearance of higher order modes. The authors also went on to suggest that there are many parameters that can have a considerable influence on the performance of bandgap fibres: choice of cladding lattice, lattice spacing, index filling fraction, choice of materials, size and shape of core defect, and structural uniformity (both in-plane and along the axis of propagation).

WO 02/075392 (Corning, Inc.) identifies a general relationship in PBG fibres between the number of so-called

surface modes that exist at the boundary between the cladding and core defect of a PBG fibre and the ratio of the radial size of the core defect and a pitch of the cladding structure,

where pitch is the centre to centre spacing of nearest
 5 neighbour holes in the triangular lattice of the exemplified cladding structure. It is suggested that when the core defect boundary, together with the photonic bandgap crystal pitch, are such that surface modes are excited or supported, a large fraction of the "light power" propagated along the fibre is
 10 essentially not located in the core defect. Accordingly, while surface states exist, the suggestion was that the distribution of light power is not effective to realise the benefits associated with the low refractive index core defect of a PBG crystal optical waveguide. The mode energy fraction
 15 in the core defect of the PBG fibre was shown to vary with increasing ratio of core defect size to pitch. In other words, it was suggested that the way to increase mode energy fraction in the core defect is by decreasing the number of surface modes, in turn, by selecting an appropriate ratio of
 20 the radial size of the core defect and a pitch of the cladding structure. In particular, WO 02/075392 states that, for a circular core structure, a ratio of core radius to pitch of around 1.07 to 1.08 provides a high mode power fraction of not less than 0.9 and is single mode. Other structures are
 25 considered, for example in Figure 7, wherein the core defect covers an area equivalent to 16 cladding holes.

In a Post-deadline paper presented at ECOC 2002, "Low Loss (13dB) Air core defect Photonic Bandgap Fibre", N. Venkataraman et al. reported a PBG fibre having a seven-cell
 30 core defect that exhibited loss as low as 13dB/km at 1500nm over a fibre length of one hundred metres. The structure of this fibre closely matches the structure considered in the book chapter referenced above. The authors attribute the

relatively small loss of the fibre as being due to the high degree of structural uniformity along the length of the fibre.

PBG fibre structures are typically fabricated by first forming a pre-form and then heating and drawing an optical fibre from that pre-form in a fibre-drawing tower. It is known either to form a pre-form by stacking capillaries and fusing the capillaries into the appropriate configuration of pre-form, or to use extrusion.

For example, in PCT/GB00/01249, identified above, a seven-cell core defect pre-form structure was formed by omitting from a stack of capillaries an inner capillary and, in addition, the six capillaries surrounding the inner capillary. The capillaries around the core defect boundary in the stack were supported during formation of the pre-form by inserting truncated capillaries, which did not meet in the middle of the stack, at both ends of the capillary stack. The stack was then heated in order to fuse the capillaries together into a pre-form suitable for drawing into an optical fibre. Clearly, only the fibre drawn from the central portion of the stack, with the missing inner seven capillaries, was suitable for use as a hollow core defect fibre.

US patent application number US 6,444,133 (Corning, Inc.), describes a technique of forming a PBG fibre pre-form comprising a stack of hexagonal capillaries in which the inner capillary is missing, thus forming a core defect of the eventual PBG fibre structure that has flat inner surfaces. In contrast, the holes in the capillaries are round. US 6,444,133 proposes that, by etching the entire pre-form, the flat surfaces of the core defect dissolve away more quickly than the curved surfaces of the outer capillaries. The effect of etching is that the edges of the capillaries that are next to the void fully dissolve, while the remaining capillaries simply experience an increase in hole-diameter. Overall, the resulting pre-form has a greater fraction of air in the

cladding structure and a core defect that is closer to a seven-cell core defect than a single cell core defect.

PCT patent application number WO 02/084347 (Corning,

Inc.) describes a method of making a pre-form comprising a
5 stack of hexagonal capillaries of which the inner capillaries
are preferentially etched by exposure to an etching agent.
Each capillary has a hexagonal outer boundary and a circular
inner boundary. The result of the etching step is that the
centres of the edges of the hexagonal capillaries around the
10 central region dissolve more quickly than the corners, thereby
causing formation of a core defect. In some embodiments, the
circular holes are offset in the inner hexagonal capillaries
of the stack so that each capillary has a wall that is thinner
than its opposite wall. These capillaries are arranged in the
15 stack so that their thinner walls point towards the centre of
the structure. An etching step, in effect, preferentially
etches the thinner walls first, thereby forming a seven-cell
core defect.

An object of the present invention is to provide a PBG
20 waveguide having improved properties, in particular lower
loss, than prior art PBG waveguides.

In arriving at the present invention, the inventors have
demonstrated that, while the size of a core defect is
significant in determining certain characteristics of a PBG
25 waveguide, the form of a boundary at the interface between
core and cladding also plays a significant role in determining
certain characteristics of the waveguide. As will be
described in detail hereafter, the inventors have determined
that, for given PBG core and cladding structures, variations
30 in only the form of the boundary can cause significant changes
in the characteristics of a respective waveguide.

According to the invention there is provided an elongate
waveguide for guiding light comprising:

a core, comprising an elongate region of relatively low refractive index; and

a photonic bandgap structure arranged to provide a photonic bandgap over a range of wavelengths of light, the structure comprising elongate regions of relatively low refractive index interspersed with elongate regions of relatively high refractive index, including a boundary region of relatively high refractive index that surrounds, in a transverse cross-section of the waveguide, the core;

characterised in that the boundary region has a shape such that, in use, light guided by the waveguide is guided in a transverse mode in which, in the transverse cross-section, more than 95% of the guided light is in the regions of relatively low refractive index in the waveguide.

In referring to the 'shape' of the boundary region, we mean 'shape' in a broad sense, both its gross shape (whether it is for example circular or hexagonal or dodecagonal or some other shape) and fine details of its shape, for example the presence or absence of local variations in thickness (for example, nodes or nodules) around its perimeter. (It is expected that the gross shape of the boundary will generally define the shape of the core.) We also use the word 'shape' to encompass the size of the boundary region; for example, we regard a boundary region that is a circular shell in the transverse plane to have a different shape for a different diameter of the shell or for a different thickness of the shell, even though it remains a circular shell in each of those cases.

The regions of relatively low refractive index in the waveguide of course comprise the regions of relatively low refractive index in the photonic bandgap structure and the region of relatively low refractive index in the core.

The inventors have discovered that in considering how best to lower loss in an optical waveguide having a photonic

bandgap cladding structure, it is helpful to consider the behaviour of distinct features in the cladding boundary as being that of optical resonators, in an approach based upon that reported in Litchinitser et al., Opt Lett., Vol. 27

5 (2002) pp. 1592-1594.

A simple example of an optical resonator is the Fabry-Perot interferometer. Whether or not light can resonate in such a feature depends on the feature's size, shape and composition, and also on the wavelength and direction of
 10 propagation of the light. As the wavelength is varied the feature moves into and out of resonance. On resonance, transmission through the feature is enhanced, causing light to concentrate in the feature to a degree determined by the feature's Q factor. If the feature is solid, concentration of
 15 light in the feature is deleterious as it decreases the proportion of light in low-index regions and increases F-factor (defined below). However, for optical frequencies in between the resonances (so-called antiresonant wavelengths) transmission through the feature is suppressed, substantially
 20 excluding light from the feature. That is advantageous as it raises the proportion of light in low-index regions and decreases F-factor. The stronger the resonances are, the more effective the antiresonances between them are at excluding light. Hence it is advantageous to incorporate features that
 25 possess strong distinct resonances, and adjust their sizes and shapes so that they are antiresonant at the optical wavelengths and directions of propagation of interest.

For example, Litchinitser et al. describe a PCF consisting of a silica core surrounded by holes filled with
 30 high index liquid. In that case the silica represents the low index medium and the filled holes are the features that act as resonators. At their antiresonant wavelengths, the filled holes substantially exclude light and thus confine light to the relatively low-index silica core. The present inventors

have considered more complicated structures, which may, for example, comprise high-index features interconnected by high index "struts", whereas the resonators described by Litchinitser et al. are isolated cylinders. Nevertheless the present inventors have discovered that such interconnected features can act as distinct resonators, and serve to confine light in the low index medium (for example, air) when they are antiresonant.

Guiding light in a region of relatively low refractive index has the advantage that losses, nonlinear effects and other material effects are generally lower in such regions, particularly if the region is a region of air or a gas. Thus, preferably in the transverse cross-section, ever more of the light may be guided in the regions of relatively low refractive index in the PBG structure or in the region of relatively low refractive index in the core: preferably more than 96%, 97%, 98%, 99%, 99.3%, 99.5% or even 99.9% of the light is in those regions.

The boundary region may have a shape such that, in use, light guided by the waveguide is guided in a transverse mode in which, in the transverse cross-section, more than 50% of the guided light is in the region of relatively low refractive index in the core. It is significant that the inventors have recognised that the light need not be in the core region for beneficial effects to be achieved. Thus, the boundary region may have a shape such that, in use, light guided by the waveguide is guided in a transverse mode in which, in the transverse cross-section, more than 1% of the guided light is in the regions of relatively low refractive index in the photonic bandgap structure. It may be that still more of the guided light is in those regions in the PBG structure: more than 2%, more than 5% or even more than 10% of the light may be in those regions.

The guided light propagating in a PBG waveguide is subject to scattering from small scale irregularities of the interfaces between higher refractive index regions and lower refractive index regions. That loss mechanism acts in addition to the Rayleigh scattering due to index inhomogeneity within the higher index regions. The latter loss mechanism is strongly suppressed in PBG waveguides having for example an air core, since most of the light power resides in air. The amount of scattering associated with the interfaces can be minimised by ensuring that impurities are eliminated during the draw process; such impurities can act as scattering (and absorption) centres directly, and can operate as nucleation sites for crystallite formation. With such imperfections removed, there still remains interface roughness governed by the thermodynamics of the drawing process. Such fluctuations are likely to be difficult or impossible to remove.

The Rayleigh scattering due to small scale roughness at the lower-index/higher-index (e.g. air-silica) interfaces can be calculated by applying a perturbation calculation. The analysis has a simple interpretation in terms of effective particulate scatterers distributed on the interfaces. If the root-mean square (RMS) height roughness is h_{rms} and the correlation lengths of the roughness along the hole direction and around the hole perimeter are L_z and L_ϕ respectively, then a typical scatterer has a volume $h_{\text{rms}}L_zL_\phi$. The induced dipole moment of the typical scatterer is then given by

$$\mathbf{p} = \Delta\epsilon \mathbf{E}_0 h_{\text{rms}} L_z L_\phi, \quad (1)$$

where $\Delta\epsilon$ is the difference in dielectric constant between the higher-index and the lower-index regions, and \mathbf{E}_0 is the E-field strength at the scatterer. That induced dipole moment radiates a power, in the free space approximation, given by

$$P_{\text{sc}} = \frac{1}{12\pi} \left(\frac{\omega}{c} \right)^4 \left(\frac{\epsilon_0}{\mu_0} \right)^{1/2} |\mathbf{p}|^2 = \frac{1}{12\pi} \left(\frac{\omega}{c} \right)^4 \Delta\epsilon^2 h_{\text{rms}}^2 L_z^2 L_\phi^2 \left(\frac{\epsilon_0}{\mu_0} \right)^{1/2} |\mathbf{E}_0|^2. \quad (2)$$

The number density of particles on the interface will be $\sim 1/(L_z L_\phi)$ so that the total radiated power from a section of length L of the perturbed fibre will be approximately

$$5 \quad P_{\text{rad}} \sim \frac{1}{12\pi} \left(\frac{\omega}{c} \right)^4 \Delta \varepsilon^2 h_{\text{rms}}^2 L_z L_\phi L \left(\frac{\varepsilon_0}{\mu_0} \right)^{1/2} \oint_{\text{perimeters}}^{\text{hole}} ds |\mathbf{E}_0|^2 \quad (3)$$

The loss rate is thus given by

$$\gamma = \frac{P_{\text{rad}}}{P_0 L} \sim \frac{1}{6\pi} \left(\frac{\omega}{c} \right)^4 \Delta \varepsilon^2 h_{\text{rms}}^2 L_z L_\phi \left(\frac{\varepsilon_0}{\mu_0} \right)^{1/2} \frac{\oint_{\text{perimeters}}^{\text{hole}} ds |\mathbf{E}_0|^2}{\int dS (\mathbf{E}_0 \wedge \mathbf{H}_0^*) \cdot \hat{\mathbf{z}}} \quad (4)$$

where the incident power P_0 has been expressed as a Poynting flux.

- 10 Equation (4) shows that the mode shape dependence of the Rayleigh interface roughness scattering strength is governed by a factor F given by

$$F = \left(\frac{\varepsilon_0}{\mu_0} \right)^{1/2} \frac{\oint_{\text{perimeters}}^{\text{hole}} ds |\mathbf{E}_0(\mathbf{r}')|^2}{\int_{\text{x-section}} dS (\mathbf{E}_0 \wedge \mathbf{H}_0^*) \cdot \hat{\mathbf{z}}} \quad (5)$$

- A comparison of the interface scattering strength from guided
15 modes of different fibres with similar interface roughness properties can be based purely on this factor. Indeed, the thermodynamic limit to surface roughness is not expected to vary significantly with the details of the fibre geometry, so that the factor F can be used directly as a figure of merit.

- 20 A more rigorous calculation of small scale interface roughness can be derived which takes into account the details on the surface roughness spectrum and deviations from the free space approximation. The latter effect is embodied by a local density of states (LDOS) correction factor appearing in the
25 integrand of the numerator integral in equation (5). Ideally, to minimise the interface loss, the field intensity of the guiding mode multiplied by the LDOS factor should be maintained as small as possible at the interfaces. In

practise, the LDOS correction is found to be small even for (silica/air) band gap fibres in comparison with the guided mode field intensity factor, so that the factor F given in expression (5) may be used to compare the interface scattering strength from guided modes of different fibre designs.

The effect of the scattering from crystallites which have formed close to the air/silica interfaces can be calculated in a similar way to the geometrical roughness considered above. Assuming the number density per unit interface length and the size of the crystallites is independent of fibre design, again F can be used directly to compare the interface scattering strengths.

The boundary region may have a shape such that, in use, light guided by the waveguide is guided in a transverse mode providing an F -factor of less than $0.23 \mu\text{m}$. That figure is calculated assuming that the waveguide guides light at a frequency of $1.55 \mu\text{m}$. For the case in which the Photonic Band Gap structure is a periodic structure having a pitch Λ , the F -factor is preferably less than $0.7 \Lambda^{-1}$.

Also according to the invention there is provided an elongate waveguide for guiding light comprising:

a core, comprising an elongate region of relatively low refractive index; and

a photonic bandgap structure arranged to provide a photonic bandgap over a range of frequencies of light, the structure comprising elongate regions of relatively low refractive index interspersed with elongate regions of relatively high refractive index, including a boundary region of relatively high refractive index that surrounds, in a transverse cross-section of the waveguide, the core;

characterised in that the boundary region has a shape such that, in use, light guided by the waveguide is guided in a transverse mode providing an F -factor of less than $0.23 \mu\text{m}$

(or, for a waveguide in which the Photonic Band Gap structure is a periodic structure having a pitch Λ , $0.7\Lambda^{-1}$).

Preferably, still lower F-factors are provided: less than $0.16 \mu\text{m}$ (or $0.5\Lambda^{-1}$ if periodic), less than $0.10 \mu\text{m}$ (or $0.3\Lambda^{-1}$ if periodic), less than $0.065 \mu\text{m}$ (or $0.2\Lambda^{-1}$ if periodic) less than $0.055 \mu\text{m}$ (or $0.17\Lambda^{-1}$ if periodic), less than $0.048 \mu\text{m}$ (or $0.15\Lambda^{-1}$ if periodic), less than $0.032 \mu\text{m}$ (or $0.10\Lambda^{-1}$ if periodic) or even less than $0.016 \mu\text{m}$ (or $0.05\Lambda^{-1}$ if periodic) are preferred.

- 10 The features next discussed may be found in embodiments of either aspect of the invention (relating to high levels of light in the relatively low refractive index regions or relating to F-factor).

In the transverse cross section, the photonic bandgap structure may comprise an array of the relatively low refractive index regions separated from one another by the relatively high refractive index regions. The array may be substantially periodic. (However, in principle, the array need not be periodic - see, for example, the paper by N. M. Litchinitser et al. discussed above. Although that paper does not provide calculations explicitly for PBG fibres, it does illustrate that photonic bandgaps may be obtained without periodicity.)

It is highly unlikely in practice that a photonic bandgap structure according to the present invention will comprise a 'perfectly' periodic array, due to imperfections being introduced into the structure during its manufacture and/or perturbations being introduced into the array by virtue of the presence of the core defect. The present invention is intended to encompass both perfect and imperfect structures. Likewise, any reference to "periodic", "lattice", or the like herein, imports the likelihood of imperfection.

The array may be a substantially triangular array. Other arrays, of course, may be used, for example, square, hexagonal or Kagomé, to name just three.

The array may have a characteristic primitive unit cell and a pitch Λ .

The boundary region may comprise, in the transverse cross-section, a plurality of relatively high refractive index boundary veins joined end-to-end around the boundary between boundary nodes, each boundary vein being joined between a leading boundary node and a following boundary node, and each boundary node being joined between two boundary veins and to a relatively high refractive index region of the photonic bandgap structure.

At least one of the boundary veins may comprise, along its length or at its end, a nodule. The nodule may have a substantially elliptical shape in the transverse cross-section, such that an ellipse having a major axis of length L and a minor axis of length W substantially fits to the shape of the nodule. The major axis may extend along the boundary vein in which the nodule is comprised.

The waveguide may guide light at a wavelength λ_1 , which may be any wavelength at which the waveguide is substantially transparent. The wavelength λ_1 may be in the ultraviolet, visible or infrared parts of the electromagnetic spectrum. The wavelength λ_1 may be in a telecoms window, for example λ_1 may be in the range 1510 nm to 1610 nm or may be in the 1300 nm band or may be in the 810 nm band.

The waveguide may be arranged to guide light at a wavelength λ_2 , wherein light guided at the wavelength λ_2 exhibits lower loss than light guided in the waveguide at any other wavelength.

The lengths of the minor and major axes of an elliptical nodule on a boundary vein have been found to be significant in increasing the fraction of light in the regions of low

refractive index and in decreasing the F-factor. In particular it has been found that, in an plane having orthogonal axes along which values of W and L are plotted, particular regions comprise particular pairs of values of W and L (represented by co-ordinates (W,L) in the plane) that provide a higher fraction of light in the regions of low refractive index, or a lower F-factor, than is found in prior-art waveguides. Table 1 sets out relations between W and L that conveniently define those particular regions. Various regions of interest may be defined more precisely by taking combinations of two or more of those relations.

Some of the relations are defined in terms of a parameter X, which is used for brevity, to reduce the number of claims necessary to cover envisaged possibilities. Thus, parameter X may be equal to the wavelength λ_1 or the wavelength λ_2 or, where the waveguide has a pitch Λ as described above, the pitch Λ .

Table 1: Relations defining preferred regions of the L-W plane.

| | |
|-------------------------|--|
| $W \approx L$ | $L \times W \approx \frac{X^2}{12}$ |
| $W \leq 0.467L$ | $L \times W \leq 0.113X^2$ |
| $W \approx \frac{L}{3}$ | $W \leq \left(\frac{1}{18} + \frac{L}{3}\right)X$ |
| $W \geq 0.238L$ | $W \geq \left(-\frac{1}{18} + \frac{L}{3}\right)X$ |
| $L \geq \frac{5X}{12}$ | $W \geq \left(\frac{5}{18} - \frac{L}{3}\right)X$ |
| $L \approx \frac{X}{2}$ | $W \leq \left(\frac{7}{18} - \frac{L}{3}\right)X$ |
| $L \leq \frac{7X}{12}$ | $W \geq (-0.133 + 0.467L)X$ |

| | |
|----------------------------|----------------------------|
| $W > \frac{X}{18}$ | $W \leq (0.095 + 0.238L)X$ |
| $W > \frac{5X}{36}$ | $W \geq (0.333 - 0.467L)X$ |
| $W \approx \frac{X}{6}$ | $W \leq (0.333 - 0.238L)X$ |
| $W \leq \frac{7X}{36}$ | $W \leq (0.467 - 0.467L)X$ |
| $L \times W \geq 0.058X^2$ | $W \leq (0.238 - 0.238L)X$ |

The core may have, in the transverse cross-section, an area that is significantly greater than the area of at least some of the relatively low refractive index regions of the photonic bandgap structure. The core may have, in the transverse cross-section, an area that is greater than twice the area of at least some of the relatively low refractive index regions of the photonic bandgap structure.

The core may have, in the transverse cross-section, an area that is greater than the area of each of the relatively low refractive index regions of the photonic bandgap structure.

The core may have, in the transverse cross-section, a transverse dimension that is greater than the pitch Λ .

The core may correspond to the omission of a plurality of unit cells of the photonic band-gap structure, for example, the core may correspond to the omission of three, four, six, seven, ten or nineteen unit cells of the photonic band-gap structure. The core may correspond to the omission of more than nineteen unit cells of the photonic band-gap structure.

At least some of the relatively low refractive index regions may be voids filled with air or under vacuum.

At least some of the relatively low refractive index regions may be voids filled with a liquid or a gas other than air. The region of relatively low refractive index that makes

up the core may comprise the same or a different material compared with the regions of relatively low refractive index in the photonic bandgap structure.

In some embodiments, at least some of the relatively high refractive index regions comprise silica glass. The glass may be un-doped or doped with index raising or lowering dopants. Alternatively, the relatively high refractive index may comprise another solid material, for example a different kind of glass or a polymer.

10 The relatively low refractive index regions may make up more than 75% by volume of the photonic bandgap structure. The relatively low refractive index regions may make around 87.5% by volume of the photonic bandgap structure.

The waveguide may support a mode having a mode profile 15 that closely resembles the fundamental mode of a standard optical fibre. An advantage of this is that the mode may readily couple into standard, single mode optical fibre.

Alternatively, or in addition, the waveguide may support a non-degenerate mode. This mode may resemble a TE_{01} mode in 20 standard optical fibres.

Preferably, in either case, said mode supports a maximum amount of the mode power in relatively low refractive index regions compared with other modes that are supported by the waveguide.

25 At least some of the boundary veins may be substantially straight. In some embodiments, substantially all of the boundary veins are substantially straight. Alternatively, or additionally, at least some of the boundary veins may be bowed outwardly from the core defect.

30 At least two of the higher index regions in the photonic bandgap structure may be connected to each other.

The higher regions in the photonic bandgap structure may be interconnected.

Also according to the invention there is provided an optical fibre comprising a waveguide of a type described above as being according to the invention.

Also according to the invention there is provided a
5 transmission line for carrying data between a transmitter and a receiver, the transmission line including along at least part of its length such a fibre.

Also according to the invention there is provided data conditioned by having been transmitted through such a
10 waveguide. As in any transmission system, data that is carried by the system acquires a characteristic 'signature' determined by a transfer function of the system. By characterising the system transfer function sufficiently accurately, using known techniques, it is possible to match a
15 model of the input data, operated on by the transfer function, with real data that is output (or received) from the transmission system.

Also according to the invention there is provided a method of forming elongate waveguide, comprising the steps:
20 forming a preform stack by stacking a plurality of elongate elements;

omitting, or substantially removing at least one elongate element from an inner region of the stack; and

heating and drawing the stack, in one or more steps, into
25 a waveguide of a type described above as being according to the invention.

Also according to the invention there is provided a method of forming elongate waveguide for guiding light, comprising the steps:

30 (a) simulating the waveguide in a computer model, the waveguide comprising a core, comprising an elongate region of relatively low refractive index and a photonic bandgap structure arranged to provide a photonic bandgap over a range of wavelengths of light, the structure comprising elongate

regions of relatively low refractive index interspersed with elongate regions of relatively high refractive index, including a boundary region of relatively high refractive index that surrounds, in a transverse cross-section of the waveguide, the core, wherein properties of the boundary region are represented in the computer model by parameters;

(b) finding a set of values of the parameters that, according to the model, increases or maximises how much of the light guided by the waveguide is in the regions of relatively low refractive index in the waveguide.

Also according to the invention, there is provided a method of forming elongate waveguide for guiding light, comprising the steps:

(a) simulating the waveguide in a computer model, the waveguide comprising a core, comprising an elongate region of relatively low refractive index, and a photonic bandgap structure arranged to provide a photonic bandgap over a range of frequencies of light, the structure comprising elongate regions of relatively low refractive index interspersed with elongate regions of relatively high refractive index, including a boundary region of relatively high refractive index that surrounds, in a transverse cross-section of the waveguide, the core, wherein properties of the boundary region are represented in the computer model by parameters;

(b) finding a set of values of the parameters that, according to the model, decreases or minimises the F-factor of the waveguide.

The boundary region may comprise, in the transverse cross-section, a plurality of relatively high refractive index boundary veins joined end-to-end around the boundary between boundary nodes, each boundary vein being joined between a leading boundary node and a following boundary node, and each boundary node being joined between two boundary veins and to a relatively high refractive index region of the photonic

bandgap structure and at least one of the boundary veins comprises, along its length, a nodule, the nodule having a ~~substantially elliptical shape in the transverse cross-~~ section, such that an ellipse having a major axis of length L and a minor axis of length W substantially fits to the shape of the nodule in the transverse cross-section, wherein the parameters for which values are found may comprise L and W.

Embodiments of the present invention will now be described, by way of example only, with reference to the accompanying drawings, of which:

Figure 1 is a diagram of a transverse cross section of a PBG fibre structure according to the invention;

Figure 2 is a diagram that illustrates how an ellipse is fitted to nodules in the structure of Fig. 1.

Figure 3 is a diagram that illustrates how various physical characteristics of PBG fibres are defined herein;

Figure 4 is a plot of fraction of light in air for a fibre according to the invention, the plot having axes showing lengths of the major axis L and the minor axis W of the ellipse of Fig. 3.

Figure 5 is a plot of F-factor for a fibre according to the invention, the plot having axes showing lengths of the major axis L and the minor axis W of the ellipse of Fig. 3.

Figure 6 is the L-W plane of Figs. 4 and 5, showing various regions of interest.

Figure 7 is a diagram of a pre-form suitable for making PBG fibre according to embodiments of the present invention;

Figure 8 is a diagram of another pre-form suitable for making a fibre according to embodiments of the present invention;

Fig. 9 is a diagram of a transverse cross section of a second PBG fibre structure according to the invention;

Fig. 10 is a plot of (i) field intensity, (ii) azimuthally averaged field intensity and (iii) distribution of

F-factor for ((a) and (b)) two orthogonal polarisation modes supported by the fibre of Fig. 9.

Fig. 11 is a diagram of a transverse cross section of a second PBG fibre structure according to the invention;

5 Fig. 12 is a diagram of a transverse cross section of a third PBG fibre structure according to the invention;

Fig. 13 is a diagram of a transverse cross section of a fourth PBG fibre structure according to the invention;

10 Fig. 14 is a diagram of a transverse cross section of a fifth PBG fibre structure according to the invention;

Fig. 15 is a schematic diagram of some examples of corral systems comprising dielectric cylinders in air (the dashed lines are used for geometric construction purposes).

Fig. 16 is a plot showing the imaginary part of the effective mode index n_{eff} for a corral system comprising six identical silica cylinders in air arranged hexagonally; the distance between the cylinders is $\Lambda=3.0, 4.5$ and $6.0\mu\text{m}$ and the wavelength is $\lambda=1.55\mu\text{m}$; $\text{Im}[n_{eff}]$, which is plotted against cylinder diameter d , is related to $\text{Im}[b]$ by $\text{Im}[n_{eff}] = \frac{\lambda \text{Im}[\beta]}{2\pi}$; also shown is $\text{Im}[b]$ for a dielectric ring of diameter $R=4.5\mu\text{m}$ vs. its thickness d .

Fig. 17 is a plot showing intensity profiles for two corral arrangements of silica cylinders at anti-resonance; the circles show the positions of the cylinder interfaces; the appearance of near nulls close to each cylinder interface is clear; the wavelength was chosen to be $\lambda=1.55\mu\text{m}$.

Fig. 18 is a plot of the imaginary part of the effective mode index n_{eff} for a corral system comprising 12 identical silica cylinders in air arranged as in the two examples shown in Fig. 17, plotted as a function of the cylinder diameter d . The wavelength is $\lambda=1.55\mu\text{m}$.

Figure 1 is a representation of a transverse cross-section of a fibre waveguide structure. In the Figure, the

black regions represent fused silica glass and the white regions represent air holes in the glass (NB: Figs. 9 and 11 to 14 are shaded the other way around, with white representing silica and black glass). As illustrated, the cladding 100 comprises a triangular array of generally hexagonal cells 105, surrounding a seven-cell core defect 110. A core defect boundary 145 is at the interface between the cladding and the core defect. The core defect boundary has twelve sides - alternating between six relatively longer sides 140 and six relatively shorter sides 130 - and is formed by omitting or removing seven central cells; an inner cell and the six cells that surround the inner cell. The cells would have typically been removed or omitted from a pre-form prior to drawing the pre-form into the fibre. As the skilled person will appreciate, although a cell comprises a void, or a hole, for example filled with air or under vacuum, the voids or holes may alternatively be filled with a gas or a liquid or may instead comprise a solid material that has a different refractive index than the material that surrounds the hole. Equally, the silica glass may be doped or replaced by a different glass or other suitable material such as a polymer.

The waveguide of Fig. 1 has a substantially periodic structure. However, as discussed above, N. M. Litchinitser et al. have demonstrated that photonic bandgaps may be achieved in non-periodic structures. The properties of the core-cladding boundary are also important in non-periodic PBG structures and the invention is not limited to substantially periodic structures but encompasses structures with some or even a high degree of aperiodicity or irregularity in the cladding structure.

Hereafter, and with reference to Figure 1, a region of glass 115 between any two holes is referred to as a "vein" and a region of glass 120 where at least three veins meet is referred to as a "node".

The core defect boundary 145 comprises the inwardly-facing veins of the innermost ring of cells that surround the core defect 110.

In practice, for triangular lattice structures that have a large air-filling fraction, for example above 75%, most of the cladding holes 105 assume a generally hexagonal form, as shown in Figure 1, and the veins are generally straight.

The cells forming the innermost ring around the boundary of the core defect, which are referred to herein as "boundary cells", have one of two general shapes. A first kind of boundary cell 125 is generally hexagonal and has an innermost vein 130 that forms a relatively shorter side of the core defect boundary 145. A second kind of boundary cell 135 has a generally pentagonal form and has an innermost vein 140 that forms a relatively longer side of the core defect boundary 145.

Referring again to Figure 1, there are twelve boundary cells 125, 135 and twelve nodes 150, which are referred to herein as "boundary nodes", around the core defect boundary 145. Specifically, as defined herein, there is a boundary node 150 wherever a vein between two neighbouring boundary cells meets the core defect boundary 145. In Figure 1, these boundary nodes 150 have slightly smaller diameters than the cladding nodes 160. Additionally, there is an enlarged region 165, "bead" or "nodule", of silica at the mid point of each relatively longer side of the core defect boundary 145. These nodules 165 coincide with the mid-point along the inner-facing vein 140 of each pentagonal boundary cell 135. The nodules 165 may result from a possible manufacturing process used to form the structure in Figure 1, as will be described in more detail below. For the present purposes, the veins 130 & 140 that make up the core defect boundary are known as "boundary veins".

As will be described below, it is possible to control the diameters of particular nodes and the existence or size of nodules along the core defect boundary during manufacture of a fibre.

5 The structure in Figure 1 and each of the following examples of different structures closely resemble practical optical fibre structures, which have either been made or may be made according to known processes or the processes described hereinafter. The structures share the following
10 common characteristics:

a pitch Λ of the cladding chosen between values of approximately $3\mu\text{m}$ and $6\mu\text{m}$ (this value may be chosen to position core-guided modes at an appropriate wavelength for a particular application);

15 a thickness t of the cladding veins of 0.0548 times the chosen pitch Λ of the cladding structure (or simply 0.0548Λ);
an air-filling fraction (AFF) in the cladding of approximately 87.5%.

The present inventors have determined that it is possible
20 to control the performance of PBG fibres in particular by aiming to maximise the amount of light that propagates in air within the fibre structure, even if some light is not in the core, in order to benefit from the properties of PBG fibres, such as reduced absorption, non-linearity and, in addition,
25 reduced mode coupling.

In particular, the inventors have identified the importance of the shape of the boundary for controlling the amount of light that propagates in air within the structure and for controlling the F-factor of the structure.

30 The core-cladding interface region of an air core PBG waveguide such as a photonic crystal fibre can be designed to exploit an anti-resonance effect to enhance the fraction of the mode power which resides in air. The geometry giving rise to the anti-resonance discussed here is based on a number of

substantially localised regions of silica (nodules 165) placed on the core surround.

As described above, Fig. 1 shows examples of locally concentrated high index regions (nodules 165) encircling an air core 110. Thin silica veins or struts 130, 140 connect the nodules together. Those struts directly connect onto to the PBG cladding region. If the struts connecting the concentrated regions of silica are thin, being less than 0.15 times the operational wavelength λ (which they are in the case of Fig. 1), then the struts connecting 130, 140 the localised high index regions do not themselves induce an anti-resonance effect; the anti-resonance is associated with substantially isolated high index regions 165. Indeed, it is found that localised regions of high index on a thin core surround can confine light better than a continuous core surround which possesses an approximately even density of silica.

The mechanism by which anti-resonance due to localised regions of high index can occur may be understood by considering a corral of high index cylinders distributed around a closed loop, which may or may not be a circle. Examples of such a geometry are shown in Fig. 15. The cylinders are everywhere surrounded by air. This system may be analysed quickly and accurately by employing a multiple scattering approach which fully exploits Mie-scattering theory; the field scattered from each cylinder is expanded in a multipole series. By applying the electromagnetic boundary conditions at the surfaces of the cylinders, an eigenvalue equation is derived. The method invokes radiating boundary conditions and can readily calculate leaky modes as well as guiding modes of the system; the former are obtained as solutions with complex β -values, with β the wavevector component along the direction of a cylinder axis. The guided modes, which are concentrated in the cylinders, satisfy

$\text{Re}[\beta] > \omega/c$, $\text{Im}[\beta] = 0$. Only leaky modes with small imaginary β components, and which therefore leak only slowly, are

retained; leakage rate is proportional to $\frac{\text{Im}[\beta]}{\text{Re}[\beta]}$ for the leaky mode solutions lies close to and just below the air light-line value ω/c .

A corral system, such as any of the examples shown in Fig. 15, is found to support an LP_{01} -like leaky mode solution, which possesses an approximately Gaussian intensity profile centred at a point p in the air region which is enclosed by the corral arrangement. Those solutions exist close to the air light line, $\beta = \omega/c$, so that the cylinders have a strong influence on the field. The cylinders force near nulls in the field intensity to occur close to their boundaries. For a given cylinder arrangement, by adjusting the size of the cylinders, the near nulls can be placed very close to the positions on the cylinder boundaries which lie closest to the point p . It is observed that $\text{Im}[\beta]$ of the leaky mode solution is minimised when this occurs, meaning that the leakage rate is minimised. That is interpreted as an anti-resonance of the corral system; anti-resonances of more simple confining systems such as a dielectric ring are also signalled by a near-null occurring very close to the innermost dielectric interface. Fig. 16^o plots $\text{Im}[\beta]$ against the cylinder diameter d for 6 cylinders evenly spaced around a circle (Fig. 16(a)), with circle radii $R=3.0$, 4.5 and $6.0\mu\text{m}$. Also shown is $\text{Im}[\beta]$ for a circular silica ring against its thickness d , for a ring radius of $R=4.5\mu\text{m}$ (Fig. 16(b)). The wavelength was set to $\lambda=1.55\mu\text{m}$. The superior confinement ability of the cylinder corral system at $R=4.5\mu\text{m}$ is clearly observed.

The confining ability of a corral system is very dependent on the number and the location of the high index regions. If the regions are too far apart, such that for the

LP₀₁-like leaky mode solution $\left| \sqrt{(\omega/c)^2 - \beta^2} \right| d$ exceeds approximately π , with d the largest separation of neighbouring high index regions in the corral, confinement will be weak. That is because the mode can resolve one or more of the gaps between the high index regions and so escape. That resolution argument can also be invoked to explain why the corral system supports far fewer leaky modes than a continuous element such as a dielectric ring. The in-plane wavevector associated with higher order modes exceeds that of the more slowly varying LP₀₁-like mode, so that in the corral system, the higher order modes are more able to resolve the gaps between the high-index regions and leak away. This is an advantage of the corral system over the continuous design; the latter will generally support more modes within and nearby the band gap region and will therefore be more subject to mode coupling loss.

Optimum confinement induced by a number of identical, parallel high-index cylinders in a corral geometry is achieved when the cylinders are evenly spaced over the circumference of a circle. The optimum number of cylinders to place around the circle depends on its radius R . The width of the anti-resonance as a function of parameters such as cylinder radius or wavelength is increased by including more cylinders, but increasing the number of cylinders beyond a certain number will weaken the confinement that can be achieved.

Although the circular corral arrangement of cylinders is optimum, the LP₀₁-like leaky mode is able to accommodate significant movement in cylinder positions without incurring much increase in loss; the field associated with this mode redistributes itself to move the near nulls of the field so that they remain close to the cylinder boundaries. The loss penalty incurred by the movement is small as long as the area of the region existing within the corral exceeds $\sim 10\lambda^2$ and the separation of neighbouring cylinders remains below the

resolution capacity of the mode. Fig. 17 (a) and (b) shows the field intensity distribution for two different arrangements of 12 identical silica cylinders. In each case, the radius of the cylinders was chosen to correspond to anti-resonance. The maintenance of the positions of nulls close to the cylinder boundaries is clearly observed. Fig. 18 compares the confinement ability of the two arrangements of 12 cylinders as a function of the cylinder diameter d . The difference in the confinement ability of the two geometries is not severe. The confinement of the 12 cylinders evenly distributed around the hexagon, shown in Fig. 17(b), is found to be virtually identical with 12 cylinders distributed evenly around a circle with an area equal to that of the hexagon.

Corral systems comprising parallel elongated elements with different shapes in cross-section, such as ellipses, will behave similarly to the cylinder case described above. The confining ability of the anti-resonance will depend upon the shape and orientation of the elements; shapes with smooth surfaces with no locally high rates of curvature can be expected to induce better confinement than shapes which possess sharp features on their surfaces. Numerical simulations of air core BG PCFs which incorporate concentrated high index regions located around the core surround have shown that the corral anti-resonance effect remains present even in such a complex geometry. As a function of a parameter such as the size of the concentrated high index regions, broad maxima are observed in the power in air fraction η and broad minima appear in the factor F given by, Eqn. 5

$$F = \left(\frac{\epsilon_0}{\mu_0} \right)^{1/2} \frac{\oint_{\text{perimeters}} dS |\mathbf{E}_0|^2}{\int_{\text{x-section}} dS (\mathbf{E}_0 \wedge \mathbf{H}_0^*) \cdot \hat{\mathbf{z}}} \quad (5)$$

The quantity F measures field intensity at the dielectric interfaces and gives a direct relative measure of the strength

of small-scale interface roughness scattering and provides an indication of the relative strength of mode coupling effects due to longer scale fluctuations. Upon examination of the LP₀₁-like mode field intensity profile at maximum η and minimum F , it is observed that near nulls occur close to the boundaries of the concentrated high index regions at locations closest to the position of peak intensity p . That confirms the mechanism in operation has the character of anti-resonance. The band gap cladding region can be interpreted as simply completing the confinement of the mode, which has already been substantially localised by the corral effect. Indeed, exploiting a corral anti-resonance can render the field intensity everywhere within the cladding to be more than 20dB below the peak intensity value. The analysis of the simple cylinder corral system presented above can be used to estimate the optimum number of concentrated elements to place around the core surround, give an indication of the size that these elements should have, and indicate the sensitivity to the parameters. Detailed numerical investigation of PBG photonic crystal fibres with concentrated index elements around the core supports this view.

The inventors have investigated the effect of varying the size of nodules. To that end, an ellipse may be fitted to the nodule. Fig. 2 shows how ellipses are fitted to nodules in a waveguide boundary region.

The light-in-air of a particular structure is directly measurable. The method of measuring light-in-air involves taking a near-field image of light as it leaves the structure, overlaying it on an SEM photograph of the structure and directly calculating the % light-in-air from the overlap of the two images.

The F-factor can also be calculated for a real fibre structure by the following method. A Scanning Electron Micrograph (SEM) is taken of the cross-sectional structure of

the fibre in question. An accurate representation of the structure, suitable for use in computer modelling, is obtained from the SEM by estimating the position of the structural

boundaries throughout the cross-section. The mode profile is

5 then calculated from the estimated structure using a computer modelling scheme described below. This provides knowledge of the electric and magnetic field distributions which enables both the numerator and denominator in Equation (5) above to be calculated.

10 The % light in air may also be calculated by superimposing the modelled mode on the modelled structure. Fig. 3 shows an idealised schematic of a portion of the fibre structure. Once the nodule is represented by an ellipse, the nodule is characterised by two parameters, the length L of the
15 ellipse's major axis and the length W of its minor axis. In the example of Fig. 1, the strut width is 0.05477λ , the length L of the fitted ellipse is 0.5λ and the length W is $0.5\lambda/3$.

Figs. 4 and 5 show how the proportion of light in air and the F-factor, respectively, of mode guided in a fibre having a
20 structure of the general form of Fig. 1 varies with the parameters L and W . In generating the plots of Figs. 4 and 5, the fibre structure of Fig. 1 was modelled on a computer and the proportion of light in air and the F-factor were calculated for various combinations of L and W . Each circle
25 in the plots of Figs 4 and 5 represents one such combination of L and W ; the diameter of the plotted circle is proportional to the proportion of light in air/F-factor, with smaller circles representing better performance, that is a higher proportion of light in air or a lower F-factor. The largest
30 circle in Figs. 4 and 5, at co-ordinate $(4\lambda/12, 4\lambda/36)$ in each plot, corresponds to a % light in air of 96.7% and an a F-factor of $0.74 \lambda^{-1}$. The smallest circle in Figs. 4 and 5, at co-ordinate $(5\lambda/12, 6\lambda/36)$ in each plot, corresponds to a % light in air of 99.3% and an a F-factor of $0.13 \lambda^{-1}$.

For the purposes of comparing aspects of the performance of various different structures it is useful to consider the modes that are supported in the band gap of various PBG fibre structures. This may be achieved by solving Maxwell's vector wave equation for the fibre structures, using known techniques. In brief, Maxwell's equations are recast in wave equation form and solved in a plane wave basis set using a variational scheme. An outline of the method may be found in Chapter 2 of the book "Photonic Crystals - Molding the Flow of Light", J.D. Joannopoulos et al., ©1995 Princeton University Press.

It can be seen that the performance is different in different regions of the plane, that is, for different values of L and W . Fig. 6 (a) and (b) show examples of lines defining various regions of the L - W plane that are believed to be of particular interest for the structure of Fig. 1. Other lines in addition to those shown in Fig. 6 may be of interest. The structure of Fig. 1 has a pitch of 3.2 microns and is designed for guiding light centred on the wavelength 1.55 microns; however the results of Figs. 4 to 6 are independent of pitch and wavelength and apply to a broad range of structures having the general form of Fig. 1.

With reference to Figure 7, fibres such as that of Fig. 1 may be made from a preform 1100 comprising a stack of hexagonal capillaries 1105. The hexagonal capillaries 1105 each have a circular bore. The cladding nodes 160 and boundary nodes 150 (from Figure 1) of the PBG fibre structure result from the significant volume of glass that is present in the preform 1100 wherever the corners 1110, 1115 of neighbouring capillaries meet. The nodules 165 are formed from the glass of the inwardly-facing corners 1120 of the capillaries that bound an inner region 1125 of the pre-form 1100, which is to become the core defect region 110 of a PBG fibre structure. These corners 1120, and the two sides of

each capillary that meet at the corners, recede due to surface tension as the stack of capillaries is heated and drawn. Such recession turns the two sides and the corner 1120 into a boundary vein 140, with a nodule 165. The inner region 1125 may be formed by omitting the inner seven capillaries from the pre-form and, for example, supporting the outer capillaries using truncated capillaries at either end of the stack, as described in PCT/GB00/01249 (described above) or by etching away glass from inner capillaries in accordance with either PCT/GB00/01249 or US 6,444,133 mentioned above.

Figure 8 illustrates another way of arranging a stack of capillaries 1200 to be drawn into a pre-form and fibre of the kind that is an embodiment of the invention. The cladding is formed by stacking round cross section capillaries 1205 in a close-packed, triangular lattice arrangement. The cladding capillaries 1205 have an outer diameter of 1.04mm and a wall thickness of 40 μ m. The inner region 1210 of the stack contains a large diameter capillary 1215 having an outer diameter of 4.46mm and a wall thickness of 40 μ m. The large diameter capillary 1215 supports the cladding capillaries while the stack is being formed and eventually becomes part of the material that forms a core defect boundary 145.

Interstitial voids 1220 that form at the locus of each close-packed, triangular group of three cladding capillaries are each packed with a glass rod 1225, which has an outer diameter of 0.498mm. The rods 1225 are inserted into the voids 1220 after the capillaries have been stacked. The rods 1225 that are packed in voids 1220 assist in forming cladding nodes 160, which have a diameter that is significantly greater than the thickness of the veins that meet at the nodes.

Omission of a rod from a void in the cladding would lead to the formation of a cladding node that has a significantly smaller diameter.

In a similar manner, rods 1230 are inserted into voids between the large-diameter capillary 1215 and between pairs of capillaries 1205 that are closest to the large diameter capillary 1215. (The triangular cladding structure naturally divides the innermost ring of capillaries 1205 into such pairs.) Rods 1230 are kept in place by thin-walled capillaries 1239. Smaller gaps 1235 formed within the pairs are not filled. Rods 1230 form, with silica from surrounding capillaries, nodules 165. The silica around gaps 1235 forms veins 130.

The stack 1200 is arranged as described with reference to Figure 8 and is then over-clad with a further, relatively thick walled capillary (not shown), which is large enough to contain the stack and, at the same time, small enough to hold the capillaries and rods in place. The entire over-clad stack is then heated and drawn into a pre-form, during which time all the interstitial voids at the boundary, and remaining voids between the glass rods and the cladding capillaries, collapse due to surface tension. The pre-form is, again, over-clad with a final, thick silica cladding and is heated and drawn into optical fibre in a known way. If surface tension alone is insufficient to collapse the interstitial voids, a vacuum may be applied to the interstitial voids of the pre-form, for example according to the process described in WO 00/49436 (The University of Bath).

In a further alternative way to form the fibre, a graphite insert is provided as an alternative to large diameter capillary 1215. The graphite insert is shaped to be a mould for the desired boundary shape. During a first drawing step, the stack of capillaries 1205 collapses onto the graphite insert and is moulded to its shape. As the partly drawn fibre cools, the graphite insert becomes loose and is removed before a second drawing step, in which the final fibre is drawn.

A further alternative way to form the fibre is by using the process described in PCT/GB00/01249 (described above), wherein the inner capillaries are replaced by truncated

capillaries, which support the outer capillaries at either end of the stack. The stack may be drawn to an optical fibre in the normal way, and the parts of the fibre incorporating the truncated capillary material may be discarded. In principle, truncated capillaries may also be used to support the stack part way along its length.

10 In another example of an embodiment of the invention (Fig. 9) a waveguide is provided having a larger core region 210. (In Fig. 9, shading is the opposite of that of Fig. 1, in that light regions correspond to silica whereas dark regions correspond to air.) Core region 210 corresponds to 19
15 unit cells of the cladding structure of the waveguide, whereas core 110 in Fig. 1 corresponds to 7 unit cells. Omission of the ring of 12 unit cells results in a different boundary from the boundary of the waveguide of Fig. 1. The boundary of the Fig. 9 waveguide has 12 longer veins 240 and 6 shorter veins
20 (in Fig. 1, there were 6 longer veins 140 and six shorter veins 130). Nodules 265 are provided on each of the longer veins 240. The nodules are elliptical in form with a major axis of length 0.5λ and a minor axis of length 0.1667λ . The cladding air filling fraction is 87.5%. Away from nodules
25 165, the core wall thickness is 0.055λ .

The performance of the structure of Fig. 9 is significantly improved over that of Fig. 1. For the 7-cell structure, best results achieved were 99.3% light in the low refractive index regions (i.e. air) and an F-factor of 0.1345
30 λ^{-1} . For the 19-cell structure, 99.7% of the light is in the low refractive index regions and the F-factor is $0.0636 \lambda^{-1}$.

Field intensity plots (Fig. 10(i) and (ii)) show that light in the two orthogonal polarisation modes ((a) and (b)) guided in the fibre is concentrated in a single-lobed pattern

(resembling the fundamental mode of a standard optical fibre, although the pattern guided in the present fibre consists of multiple transverse modes) that is mostly concentrated in the core 210. Fig. 10 (iii) shows the distribution of F-factor, that is, which air-silica boundaries are contributing most to the F-factor. A bright pixel shows a section of boundary that is interacting with a high intensity part of the field. The plots demonstrate that there is significant overlap of the light in the guided mode with the core boundary and illustrate the importance of nodule dimensions.

Other PBG waveguides having different PBG boundary shapes are shown in Figs. 11 to 14. In Fig. 11, nodules 365 are at the mid-points of the longer veins, as in previously described embodiments, but in this case are semi-elliptical in shape, being flat on the surface of the vein furthest from the core and elliptical on the surface of the vein closest to the core. Conversely, in Fig. 12, nodules 465 are semi-elliptical in shape, being flat on the surface of the vein closest to the core and elliptical on the surface of the vein furthest from the core.

In the embodiment of Fig. 13, the waveguide has a 'nineteen-cell' core, as in Fig. 9, but in this case the nodules 565 are nodes joining pairs of longer veins at their ends and also joining them to other parts of the photonic band-gap structure.

In the embodiment of Fig. 14, the waveguide again has a 'nineteen-cell core', but in this case the nodules 656 are provided from the six shortest veins in the boundary region.

It will thus be understood that the nodules may take any suitable form and location in the boundary. For example, the nodules need not be at the mid-point of a vein and may indeed be at a node joining two veins. Furthermore, the nodules need not be elliptical or circular in cross-section; they may for example be 'lumpy', for example a 'double lump' may be made by

fusing two side-by-side rods together during drawing of the fibre.

The skilled person will appreciate that the various structures described above may be manufactured using the

5 described manufacturing process or a prior art processes. For example, rather than using a stacking and drawing approach to manufacture, a pre-form may be made using a known extrusion process and then that pre-form may be drawn into an optical fibre in the normal way.

10 In addition, the skilled person will appreciate that while the examples provided above relate exclusively to PBG fibre cladding structures comprising triangular arrays, the present invention is in no way limited to such cladding structures. For example, the invention could relate equally
15 to square lattice structures, or structures that are not close-packed. In general, the inventors propose that given a cladding structure that provides a PBG and a core defect in the cladding structure that supports guided modes, the form of the boundary at the interface between the core defect and the
20 cladding structure will have a significant impact on the characteristics of the waveguide, as described herein.

The skilled person will appreciate that the structures described herein fit on a continuum comprising a huge number of different structures, for example having different
25 combinations of core defect size, boundary node size, boundary vein thickness and, in general, boundary and cladding form. Clearly, it would be impractical to illustrate each and every variant of PBG waveguide structure herein. As such, the skilled person will accept that the present invention is
30 limited in scope only by the present claims.

CLAIMS

1. An elongate waveguide for guiding light comprising:
a core, comprising an elongate region of relatively low
5 refractive index; and
a photonic bandgap structure arranged to provide a
photonic bandgap over a range of wavelengths of light, the
structure comprising elongate regions of relatively low
refractive index interspersed with elongate regions of
10 relatively high refractive index, including a boundary region
of relatively high refractive index that surrounds, in a
transverse cross-section of the waveguide, the core;
characterised in that the boundary region has a shape
such that, in use, light guided by the waveguide is guided in
15 a transverse mode in which, in the transverse cross-section,
more than 95% of the guided light is in the regions of
relatively low refractive index in the waveguide.
2. A waveguide as claimed in claim 1, in which the boundary
region has a shape such that, in use, light guided by the
20 waveguide is guided in a transverse mode in which, in the
transverse cross-section, more than 1% of the guided light is
in the regions of relatively low refractive index in the
photonic bandgap structure.
3. A waveguide as claimed in any preceding claim, in which
25 the boundary region has a shape such that, in use, light
guided by the waveguide is guided in a transverse mode in
which, in the transverse cross-section, more than 50% of the
guided light is in the region of relatively low refractive
index in the core.
- 30 4. A waveguide as claimed in any preceding claim, in which
the boundary region has a shape such that, in use, light
guided by the waveguide is guided in a transverse mode
providing an F-factor of less than $0.23 \mu\text{m}$.
5. An elongate waveguide for guiding light comprising:

a core, comprising an elongate region of relatively low refractive index; and

a photonic bandgap structure arranged to provide a photonic bandgap over a range of frequencies of light, the structure comprising elongate regions of relatively low refractive index interspersed with elongate regions of relatively high refractive index, including a boundary region of relatively high refractive index that surrounds, in a transverse cross-section of the waveguide, the core;

characterised in that the boundary region has a shape such that, in use, light guided by the waveguide is guided in a transverse mode providing an F-factor of less than $0.23 \mu\text{m}$.

6. A waveguide as claimed in any preceding claim, in which in the transverse cross section, the photonic bandgap structure comprises an array of the relatively low refractive index regions separated from one another by the relatively high refractive index regions.

7. A waveguide as claimed in claim 6, in which the array is substantially periodic.

8. A waveguide as claimed in claim 6 or claim 7, in which the array is a substantially triangular array.

9. A waveguide as claimed in any of claims 6 to 8, in which the array has a characteristic primitive unit cell and a pitch Λ .

10. A waveguide as claimed in any preceding claim, in which the boundary region comprises, in the transverse cross-section, a plurality of relatively high refractive index boundary veins joined end-to-end around the boundary between boundary nodes, each boundary vein being joined between a leading boundary node and a following boundary node, and each boundary node being joined between two boundary veins and to a relatively high refractive index region of the photonic bandgap structure.

11. A waveguide as claimed in claim 10, in which at least one of the boundary veins comprises, along its length or at its end, a nodule.
12. A waveguide as claimed in claim 11, in which the nodule
5 has a substantially elliptical shape in the transverse cross-section, such that an ellipse having a major axis of length L and a minor axis of length W substantially fits to the shape of the nodule in the transverse cross-section.
13. A waveguide as claimed in claim 12, in which the major
10 axis extends along the boundary vein in which the nodule is comprised.
14. A waveguide as claimed in claim 12 or 13, in which the lengths of the minor and major axes are substantially equal, that is $W \approx L$.
- 15 15. A waveguide as claimed in claim 12 or 13, in which
 $W \leq 0.467L$.
16. A waveguide as claimed in claim 15, in which the length of the minor axis is substantially equal to one-third of the length of the major axis, that is $W \approx \frac{L}{3}$.
- 20 17. A waveguide as claimed in any of claims 12 to 16, in which $W \geq 0.238L$.
18. A waveguide as claimed in claim 12 or claim 13, arranged to guide light at a wavelength λ_1 , which is in the ultraviolet, visible or infrared parts of the electromagnetic spectrum.
- 25 19. A waveguide as claimed in any of claims 12 to 18, arranged to guide light at a wavelength λ_2 , wherein light guided at the wavelength λ_2 exhibits lower loss than light guided in the waveguide at any other wavelength.
20. A waveguide as claimed in claim 18 or 19, there being a
30 parameter X that is equal to the wavelength λ_1 or the wavelength λ_2 .

21. A waveguide as claimed in any of claims 12 to 19, when dependent on claim 9, there being a parameter X that is equal to the wavelength λ_1 , the wavelength λ_2 or the pitch Λ .

22. A waveguide as claimed in claim 20 or 21, in which $L \geq \frac{5X}{12}$.

5 23. A waveguide as claimed in claim 22, in which the length of the major axis is substantially equal to half the pitch, that is $L \approx \frac{X}{2}$.

24. A waveguide as claimed in any of claims 20 to 23, in which $L \leq \frac{7X}{12}$.

10 25. A waveguide as claimed in any of claims 20 to 24, in which $W > \frac{X}{18}$.

26. A waveguide as claimed in claim 25, in which $W > \frac{5X}{36}$.

27. A waveguide as claimed in claim 26, in which the length of the minor axis is substantially equal to one-sixth of the
15 pitch, that is $W \approx \frac{X}{6}$.

28. A waveguide as claimed in any of claims 20 to 27, in which $W \leq \frac{7X}{36}$.

29. A waveguide as claimed in any of claims 20 to 28, in which $L \times W \geq 0.058X^2$.

20 30. A waveguide as claimed in claim 29, in which the product of the lengths of the major and minor axes is substantially equal to one-twelfth the square of the pitch, that is

$$L \times W \approx \frac{X^2}{12}.$$

31. A waveguide as claimed in any of claims 20 to claim 30,
25 in which $L \times W \leq 0.113X^2$.

32. A waveguide as claimed in any of claims 20 to claim 31,
in which $W \leq \left(\frac{1}{18} + \frac{L}{3} \right) X$.

33. A waveguide as claimed in any of claims 20 to claim 32,
in which $W \geq \left(-\frac{1}{18} + \frac{L}{3} \right) X$.

5 34. A waveguide as claimed in any of claims 20 to claim 33,
in which $W \geq \left(\frac{5}{18} - \frac{L}{3} \right) X$.

35. A waveguide as claimed in any of claims 20 to claim 34,
in which $W \leq \left(\frac{7}{18} - \frac{L}{3} \right) X$.

36. A waveguide as claimed in any of claims 20 to claim 35,
10 in which $W \geq (-0.133 + 0.467L)X$.

37. A waveguide as claimed in any of claims 20 to claim 36,
in which $W \leq (0.095 + 0.238L)X$.

38. A waveguide as claimed in any of claims 20 to claim 37,
in which $W \geq (0.333 - 0.467L)X$.

15 39. A waveguide as claimed in any of claims 20 to claim 38,
in which $W \leq (0.333 - 0.238L)X$.

40. A waveguide as claimed in any of claims 20 to claim 39,
in which $W \leq (0.467 - 0.467L)X$.

41. A waveguide as claimed in any of claims 20 to claim 40,
20 in which $W \leq (0.238 - 0.238L)X$.

42. A waveguide as claimed in any preceding claim, in which
the core has, in the transverse cross-section, an area that is
significantly greater than the area of at least some of the
relatively low refractive index regions of the photonic
25 bandgap structure.

43. A waveguide as claimed in claim 42, in which the core
has, in the transverse cross-section, an area that is greater
than twice the area of at least some of the relatively low
refractive index regions of the photonic bandgap structure.

44. A waveguide as claimed in any preceding claim, in which the core has, in the transverse cross-section, an area that is greater than the area of each of the relatively low refractive index regions of the photonic bandgap structure.

5 45. A waveguide as claimed in any preceding claim, in which at least some of the relatively low refractive index regions are voids filled with air or under vacuum.

46. A waveguide as claimed in any preceding claim, in which at least some of the relatively low refractive index regions
10 are voids filled with a gas other than air or a liquid.

47. A waveguide as claimed in any preceding claim, in which at least some of the relatively high refractive index regions comprise silica glass.

48. A waveguide as claimed in any preceding claim, in which
15 the relatively low refractive index regions make up more than 75% by volume of the photonic bandgap structure.

49. A waveguide as claimed in claim 48, in which the relatively low refractive index regions make around 87.5% by volume of the photonic bandgap structure.

20 50. A waveguide as claimed in any preceding claim, in which at least two of the higher index regions in the photonic bandgap structure are connected to each other.

51. A waveguide as claimed in claim 50, in which the higher regions in the photonic bandgap structure are interconnected.

25 52. An optical fibre comprising a waveguide as claimed in any preceding claim.

53. A transmission line for carrying data between a transmitter and a receiver, the transmission line including along at least part of its length a fibre as claimed in claim

30 52.

54. Data conditioned by having been transmitted through a waveguide as claimed in any of claims 1 to 51.

55. A method of forming elongate waveguide, comprising the steps:

forming a preform stack by stacking a plurality of elongate elements;

omitting, or substantially removing at least one elongate element from an inner region of the stack; and

5 heating and drawing the stack, in one or more steps, into a waveguide according to any of claims 1 to 51.

56. A method of forming elongate waveguide for guiding light, comprising the steps:

(a) simulating the waveguide in a computer model, the
10 waveguide comprising a core, comprising an elongate region of relatively low refractive index and a photonic bandgap structure arranged to provide a photonic bandgap over a range of wavelengths of light, the structure comprising elongate
15 elongate regions of relatively low refractive index interspersed with elongate regions of relatively high refractive index, including a boundary region of relatively high refractive index that surrounds, in a transverse cross-section of the waveguide, the core, wherein properties of the boundary region are represented in the computer model by parameters;

20 (b) finding a set of values of the parameters that, according to the model, increases or maximises how much of the light guided by the waveguide is in the regions of relatively low refractive index in the waveguide.

57. A method of forming elongate waveguide for guiding light,
25 comprising the steps:

(a) simulating the waveguide in a computer model, the waveguide comprising a core, comprising an elongate region of relatively low refractive index, and a photonic bandgap structure arranged to provide a photonic bandgap over a range
30 of frequencies of light, the structure comprising elongate regions of relatively low refractive index interspersed with elongate regions of relatively high refractive index, including a boundary region of relatively high refractive index that surrounds, in a transverse cross-section of the

waveguide, the core, wherein properties of the boundary region are represented in the computer model by parameters;

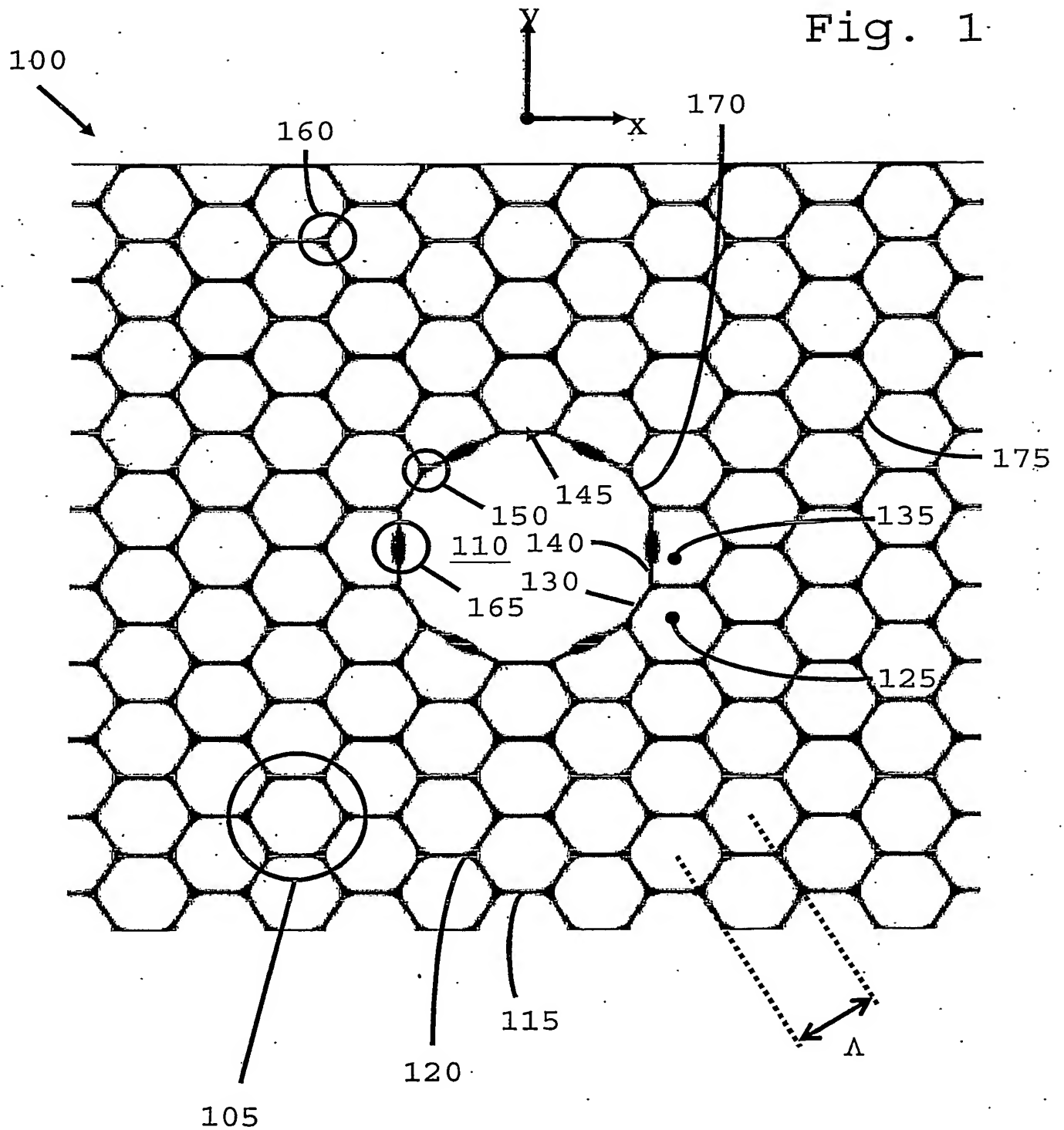
(b) finding a set of values of the parameters that,

according to the model, decreases or minimises the F-factor of
5 the waveguide.

58. A method as claimed in claim 56 or 57, in which the boundary region comprises, in the transverse cross-section, a plurality of relatively high refractive index boundary veins joined end-to-end around the boundary between boundary nodes,
10 each boundary vein being joined between a leading boundary node and a following boundary node, and each boundary node being joined between two boundary veins and to a relatively high refractive index region of the photonic bandgap structure and at least one of the boundary veins comprises, along its
15 length, a nodule, the nodule having a substantially elliptical shape in the transverse cross-section, such that an ellipse having a major axis of length L and a minor axis of length W substantially fits to the shape of the nodule in the transverse cross-section, wherein the parameters for which
20 values are found comprise L and W .

59. An optical waveguide substantially as hereinbefore described, with reference to the accompanying drawings.

Fig. 1



2/17

Fig. 2

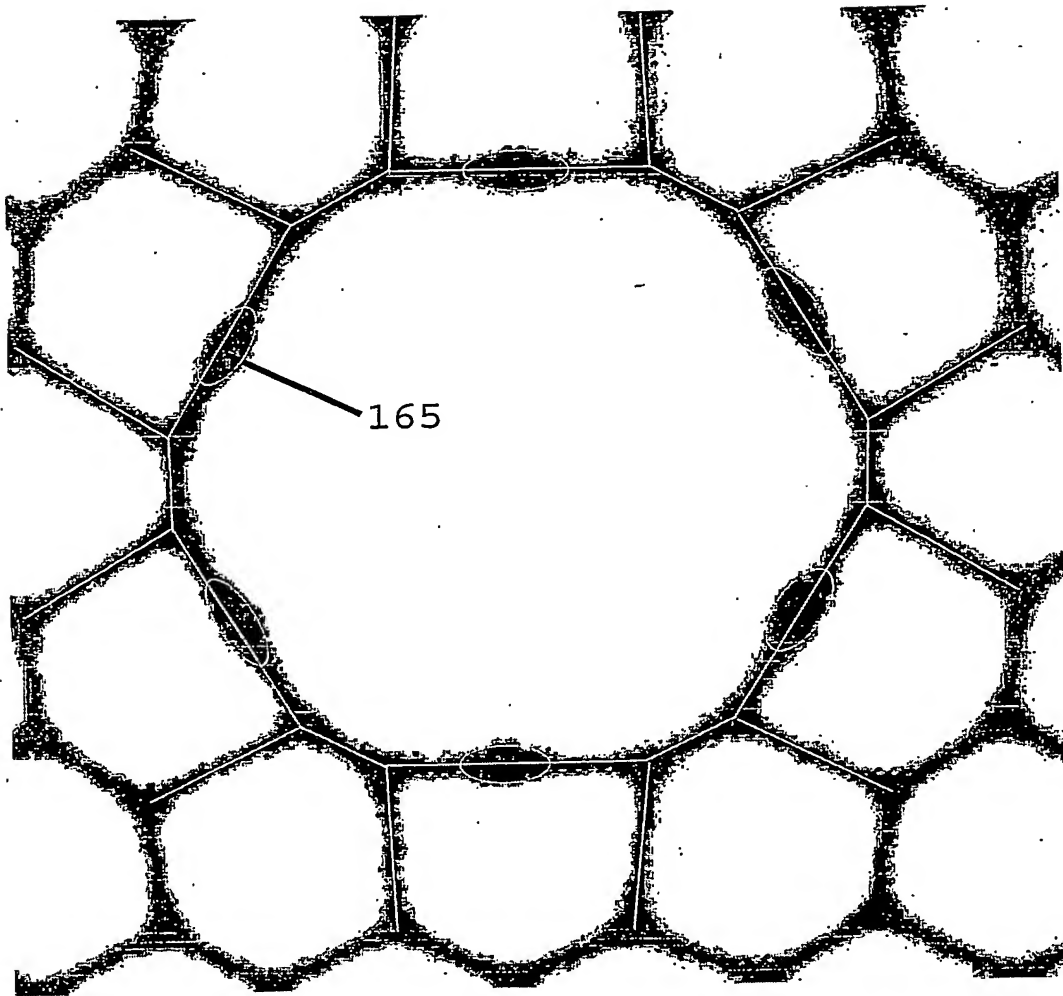
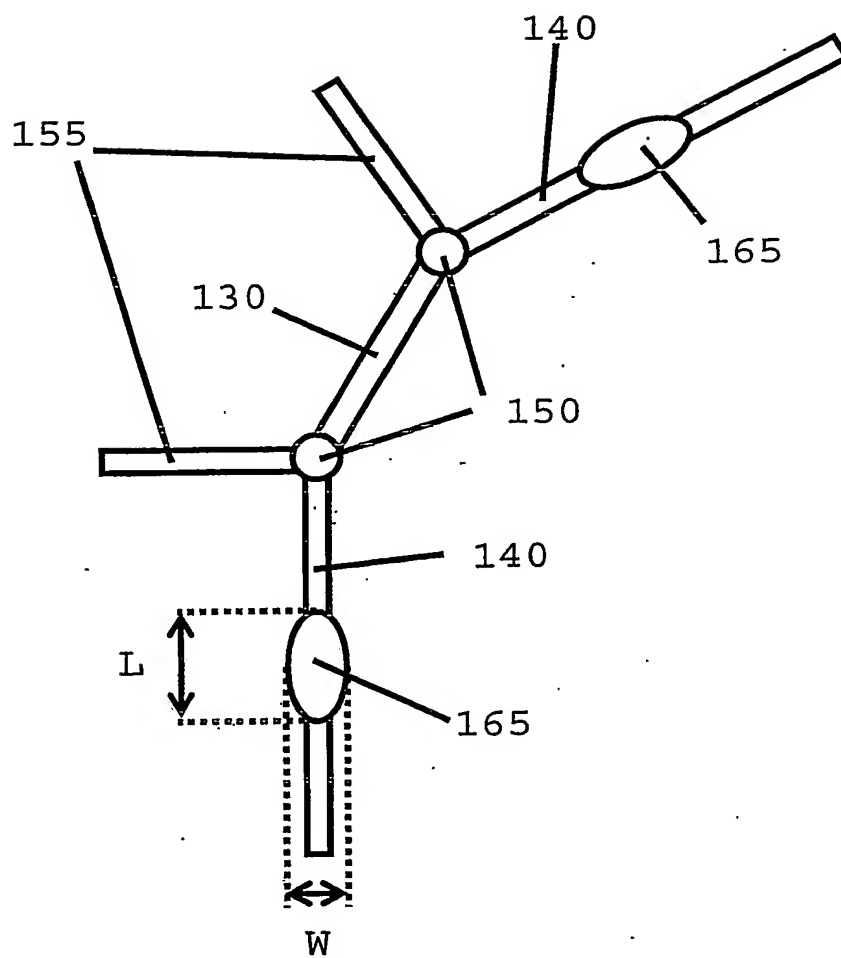
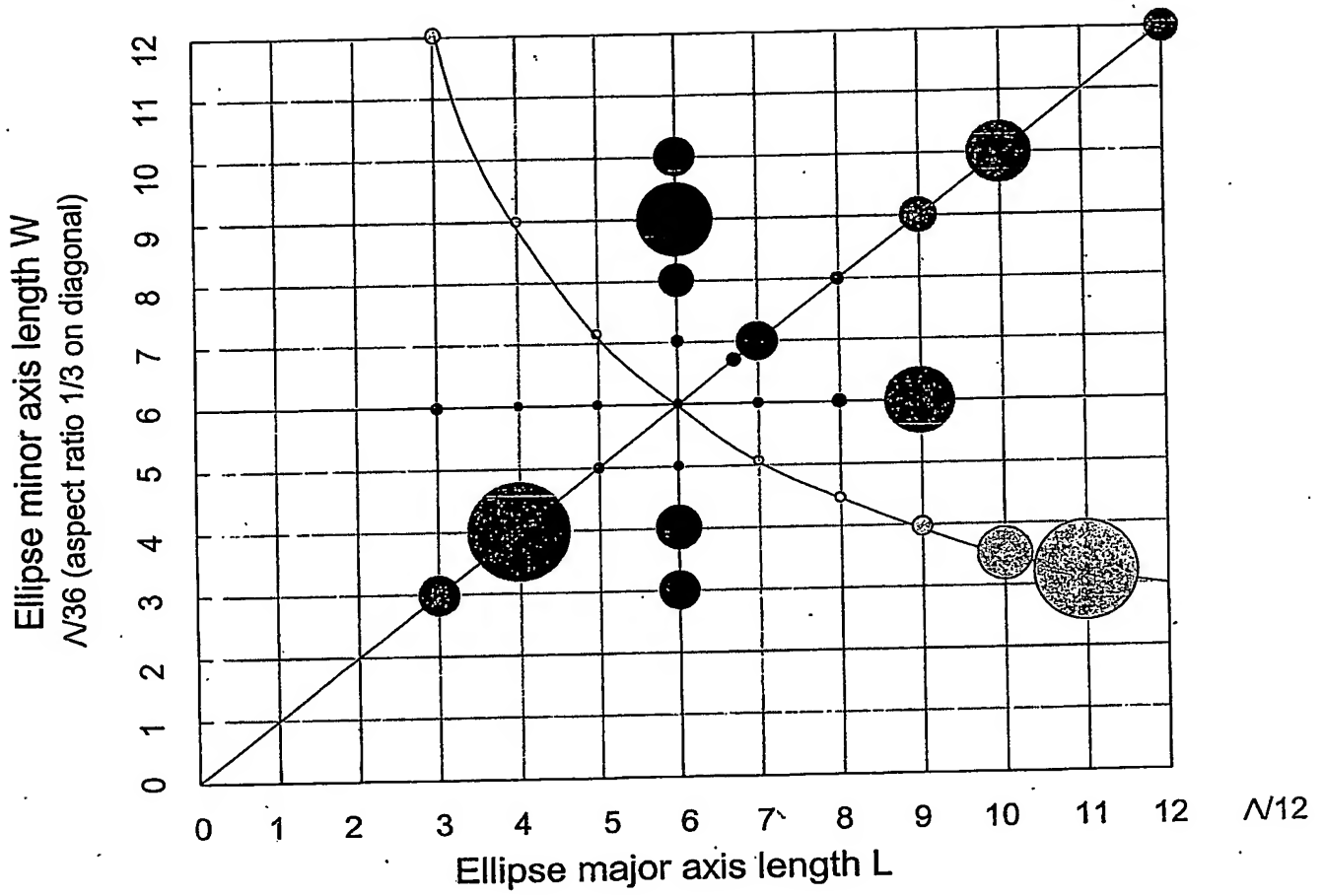


Fig. 3



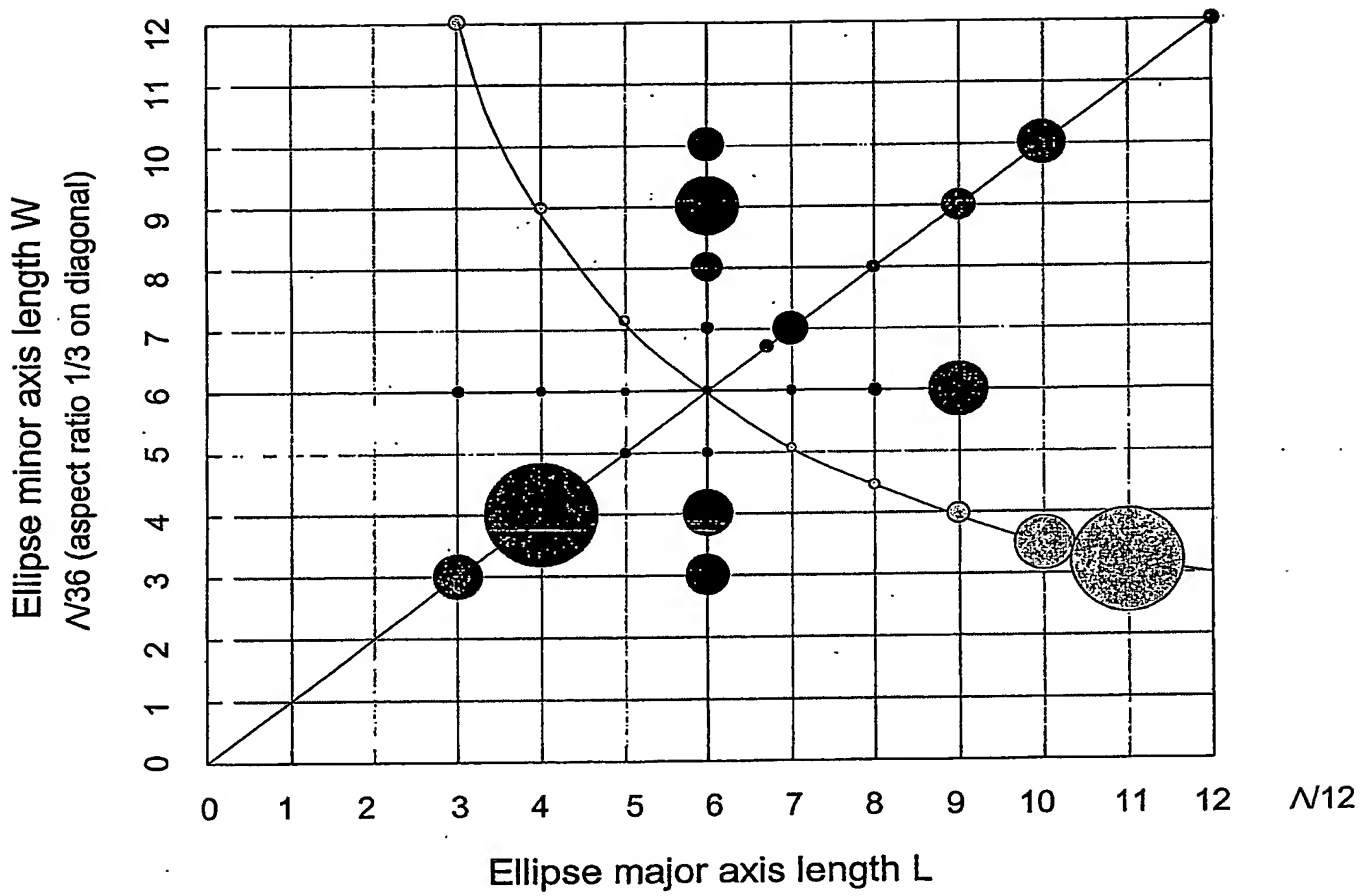
4/17

Fig. 4



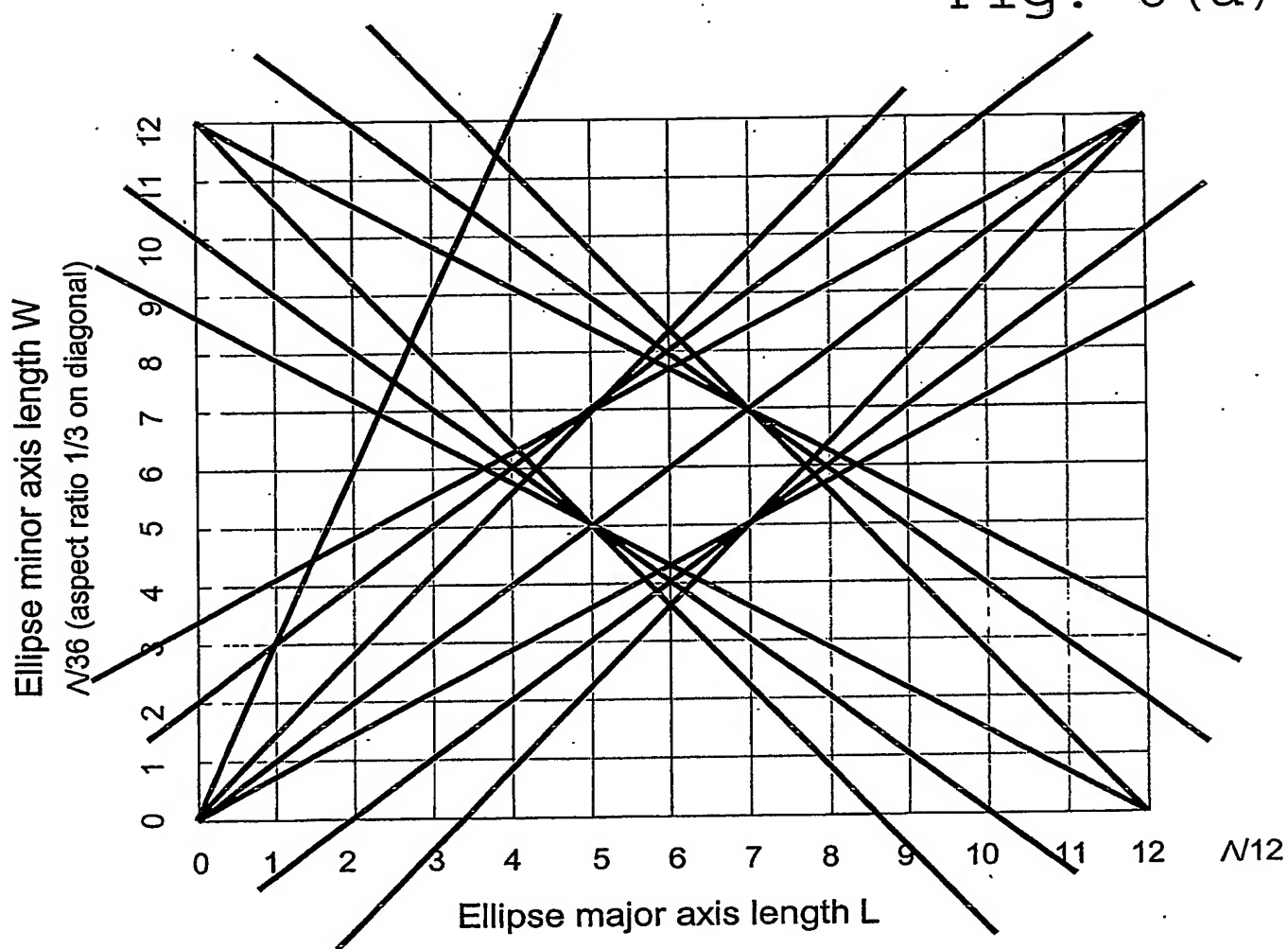
5/17

Fig. 5



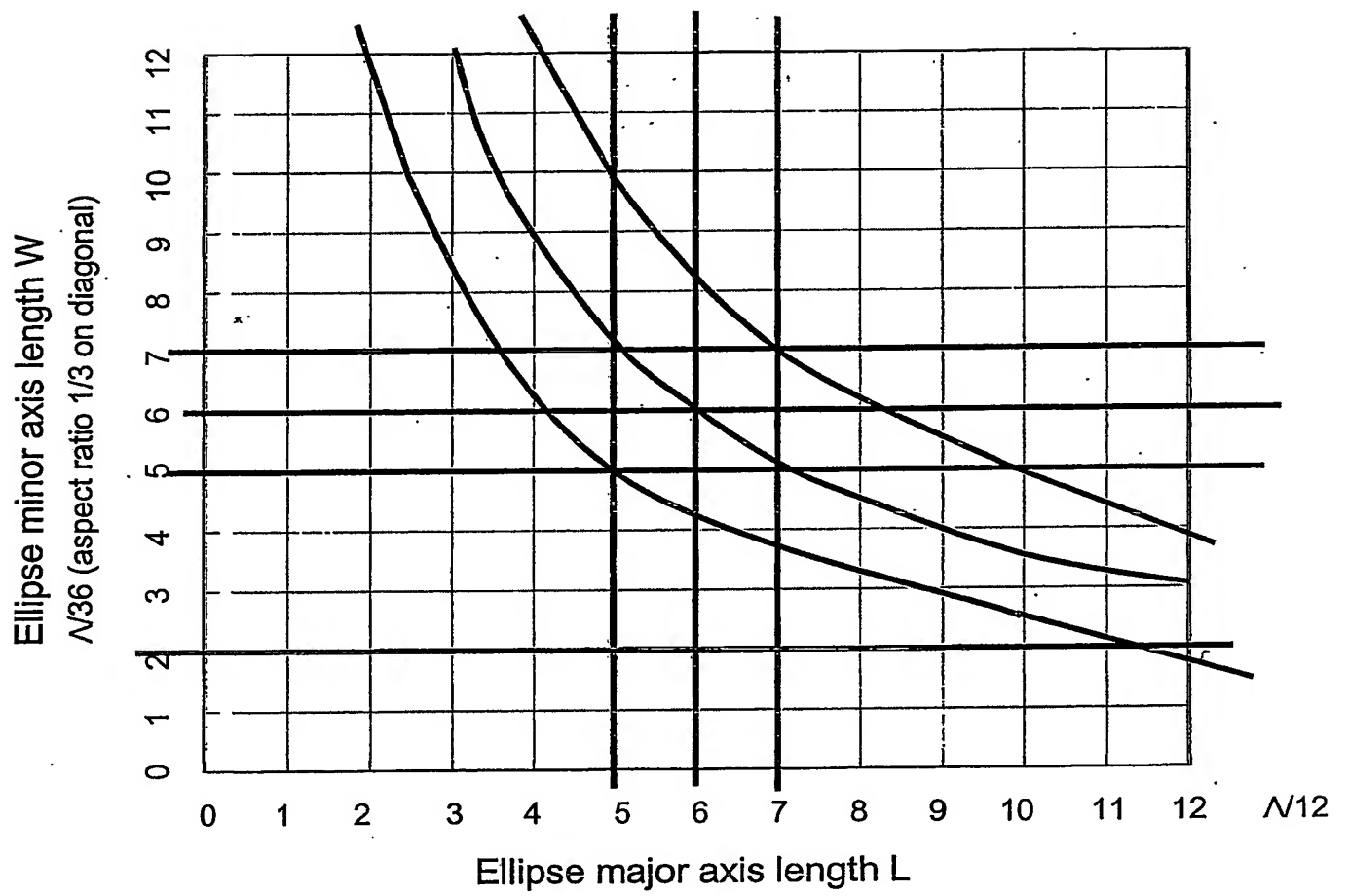
6/17

Fig. 6(a)



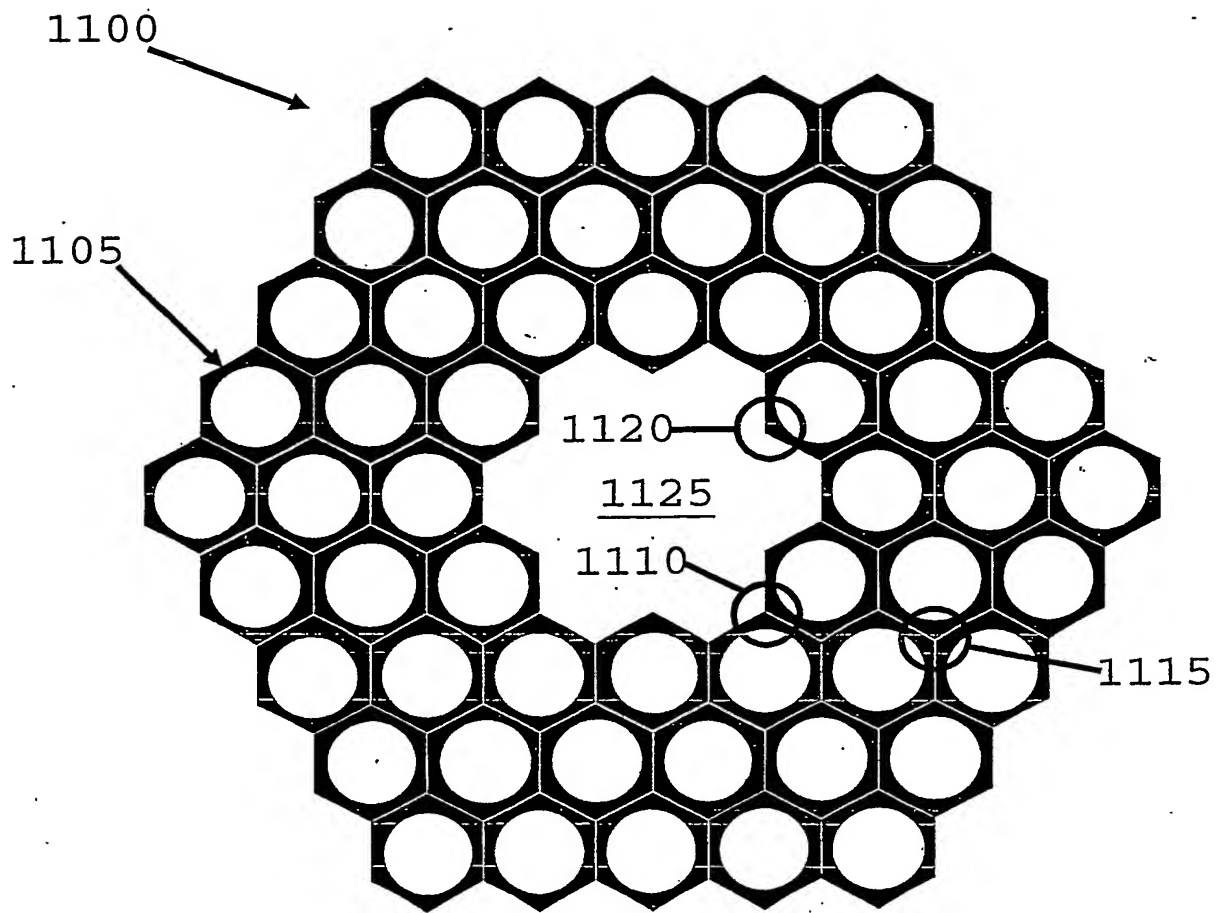
7/17

Fig. 6 (b)



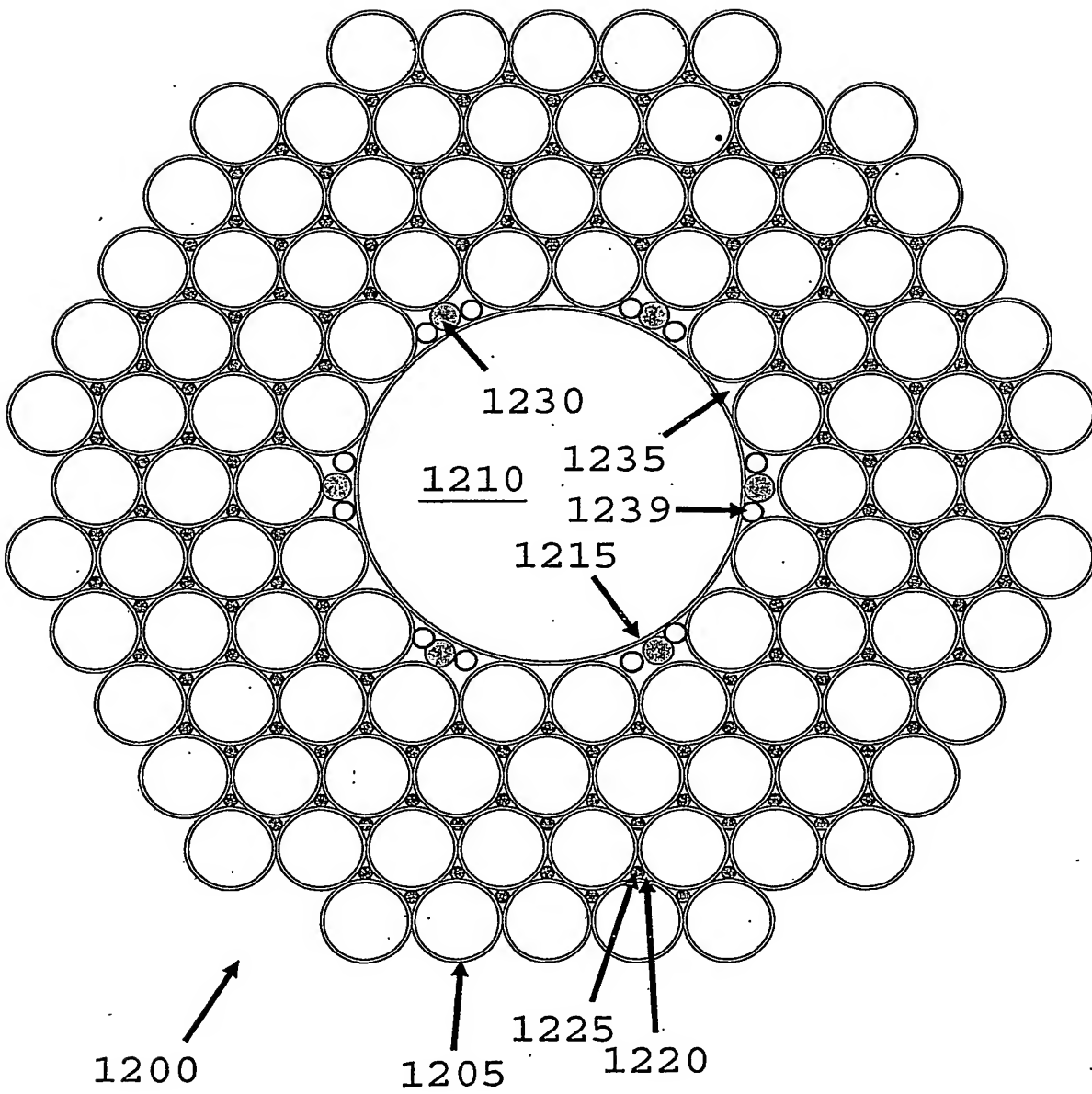
8/17

Fig. 7



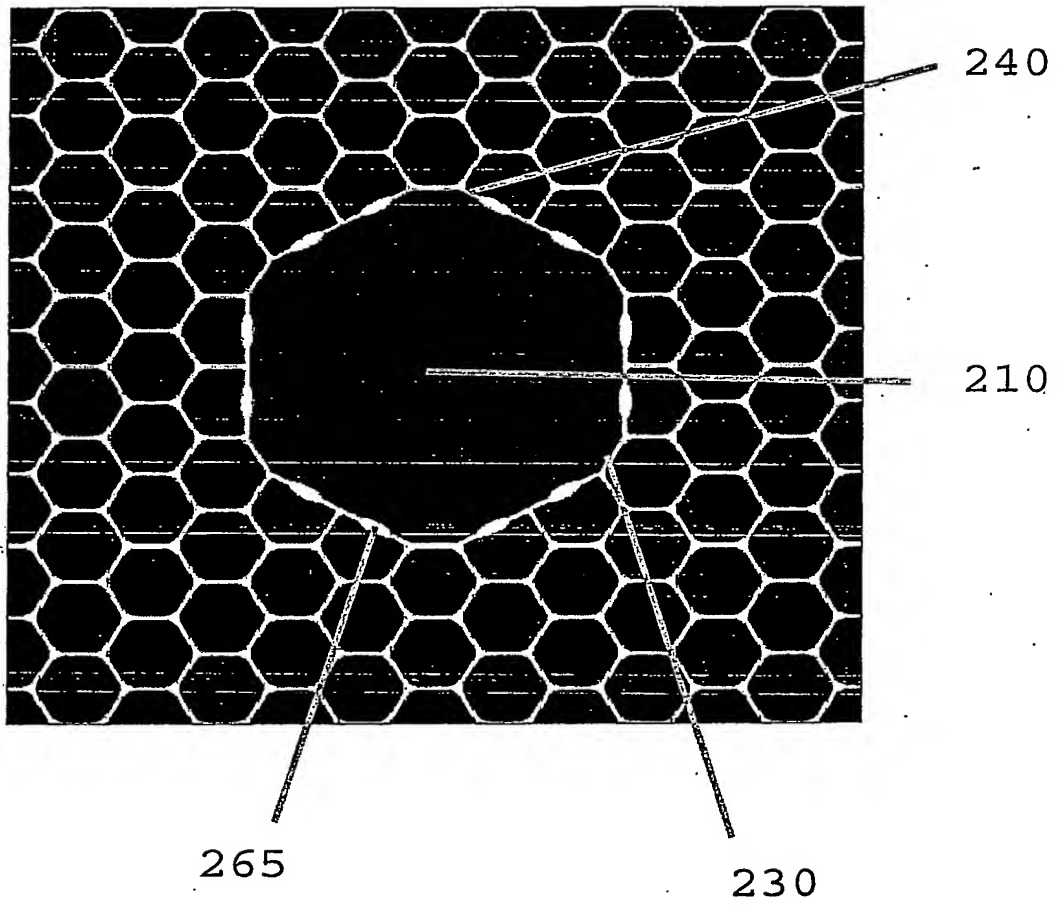
9/17

Fig. 8



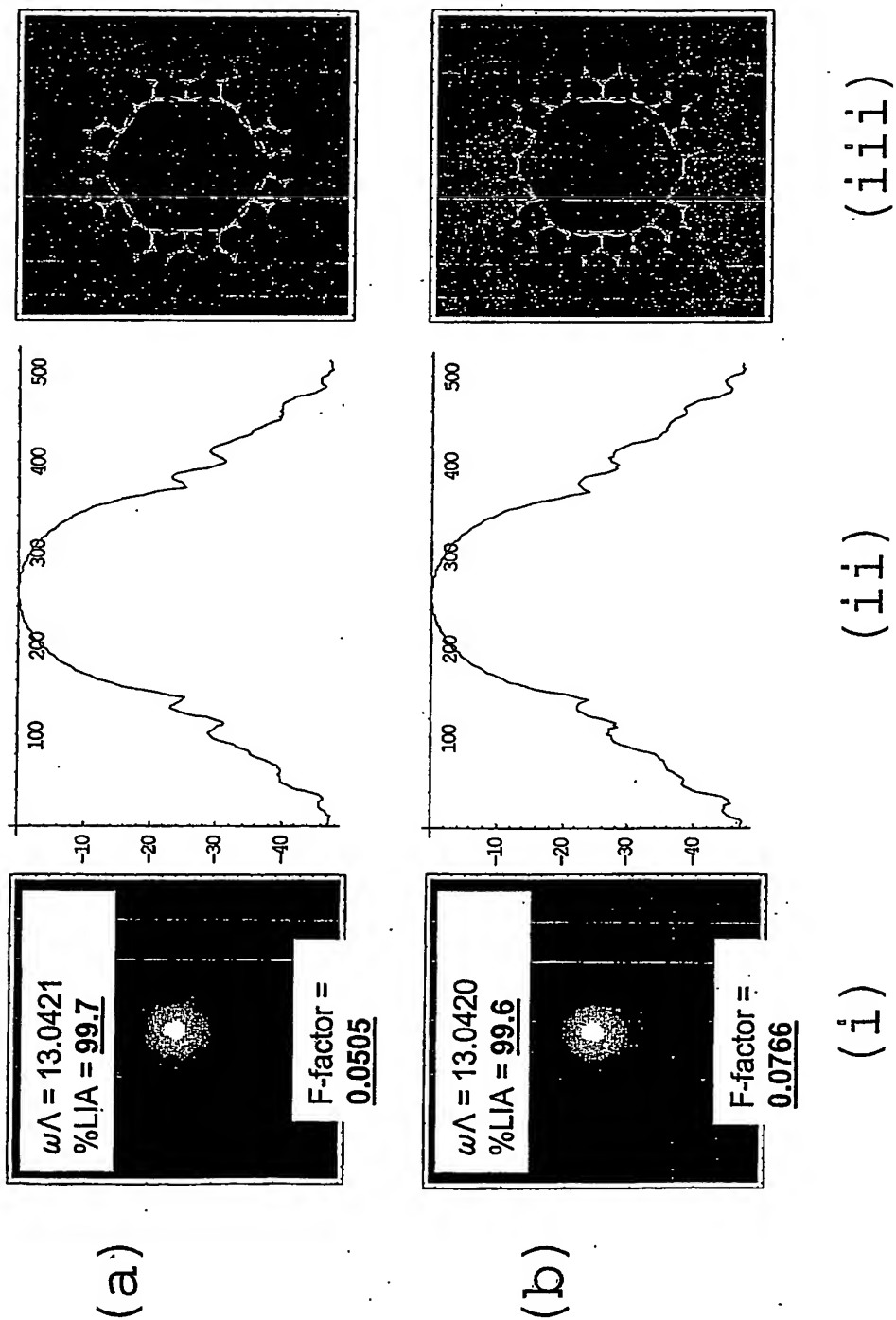
10/17

Fig. 9



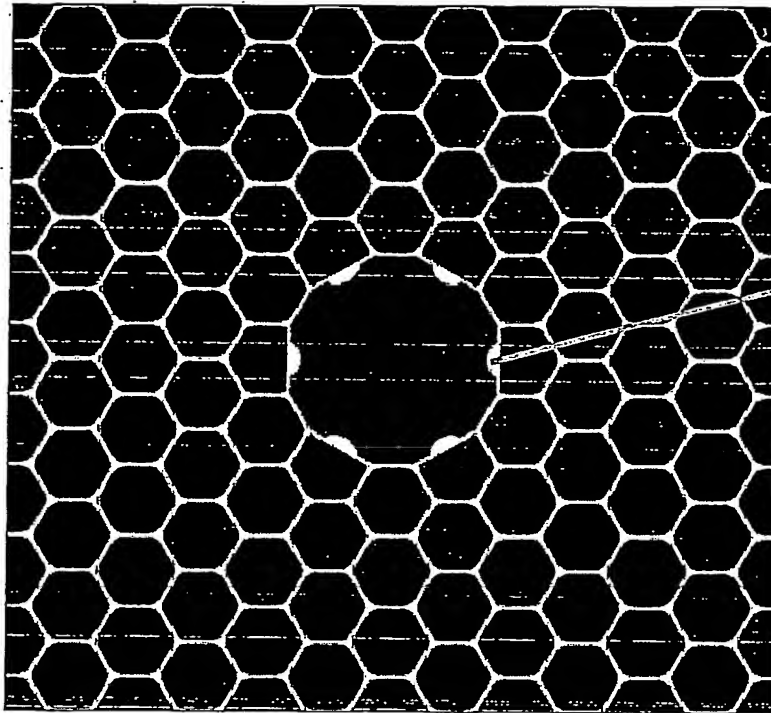
11/17

Fig. 10



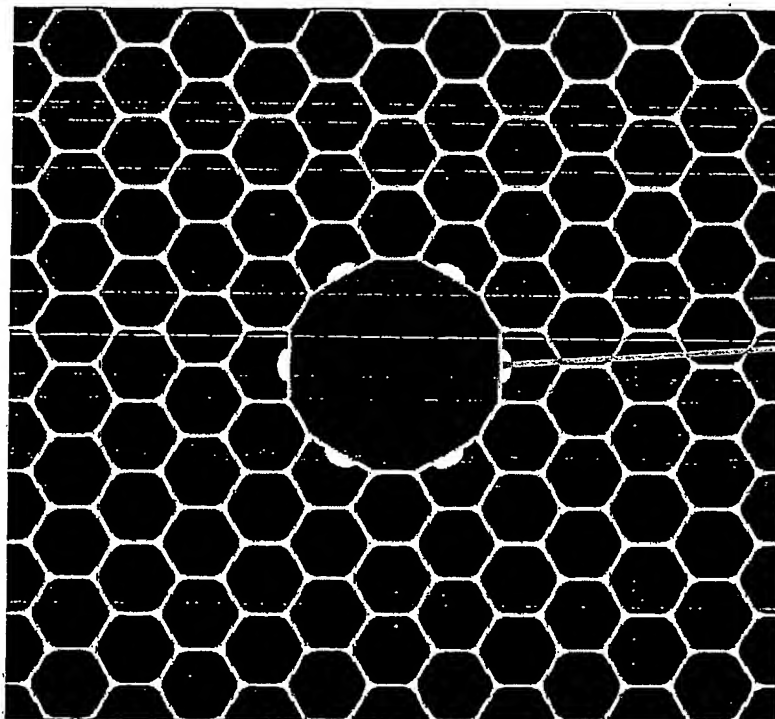
12/17

Fig. 11



365

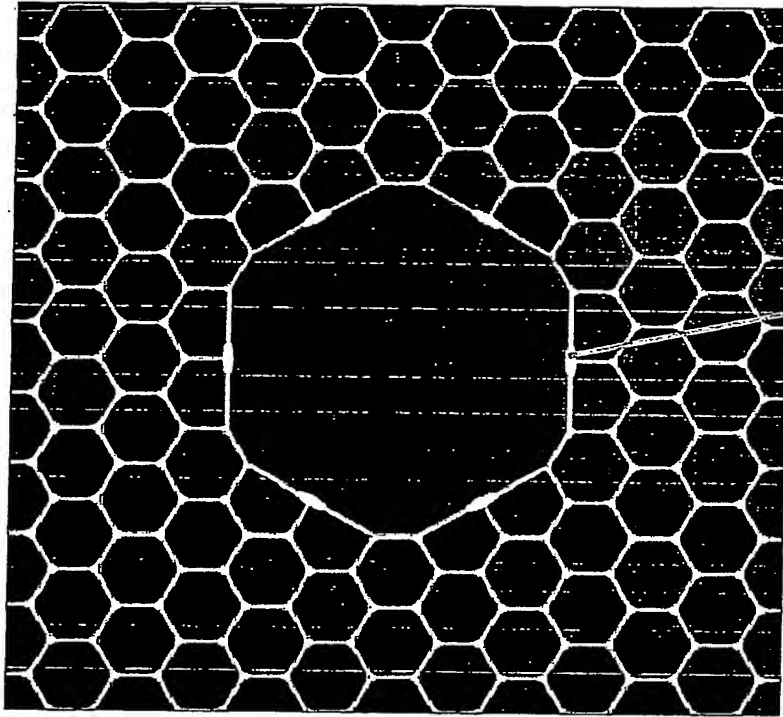
Fig. 12



465

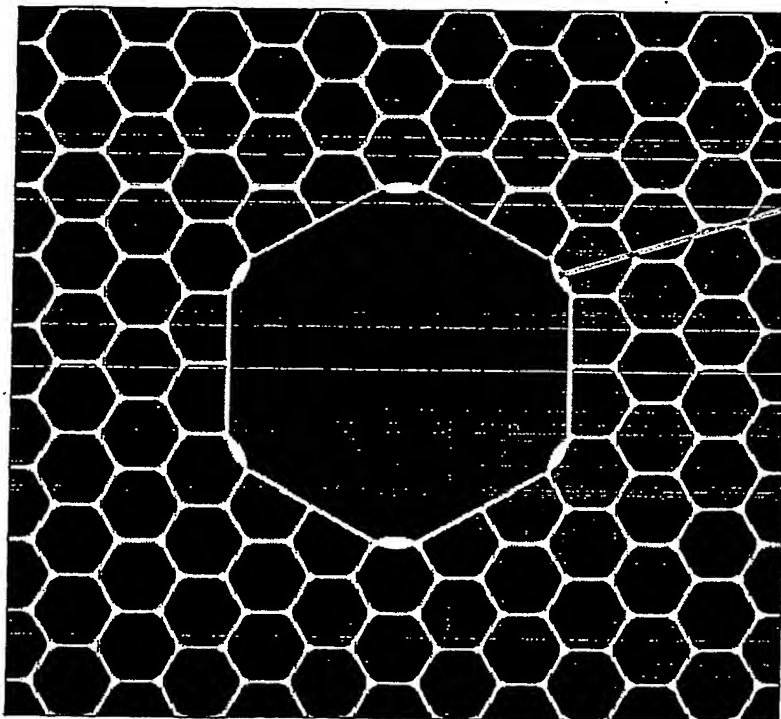
13/17

Fig. 13



565

Fig. 14



665

14/17

Fig. 15

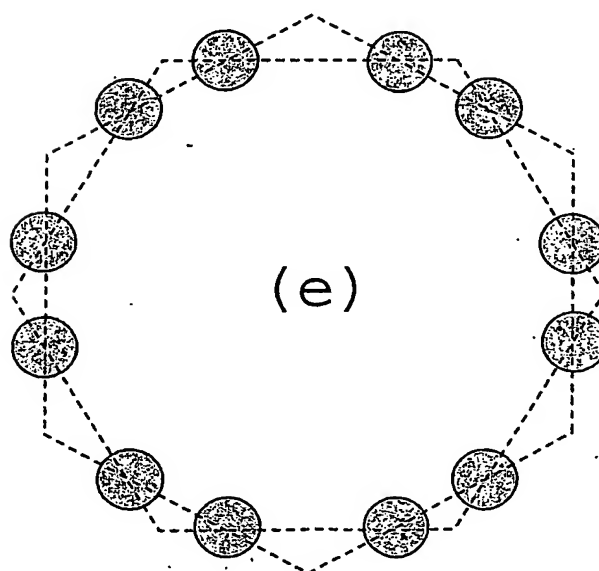
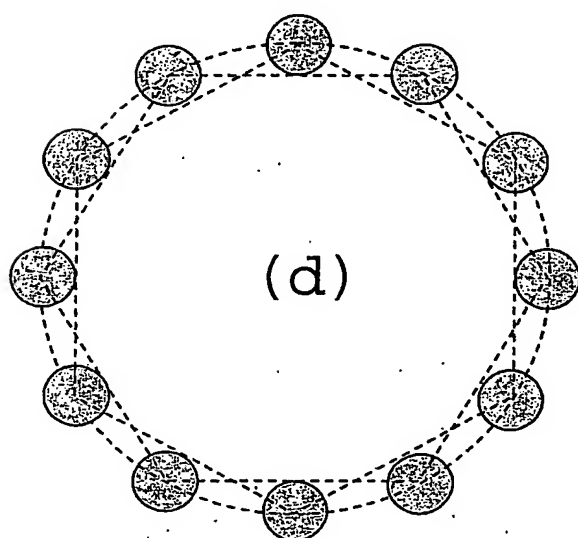
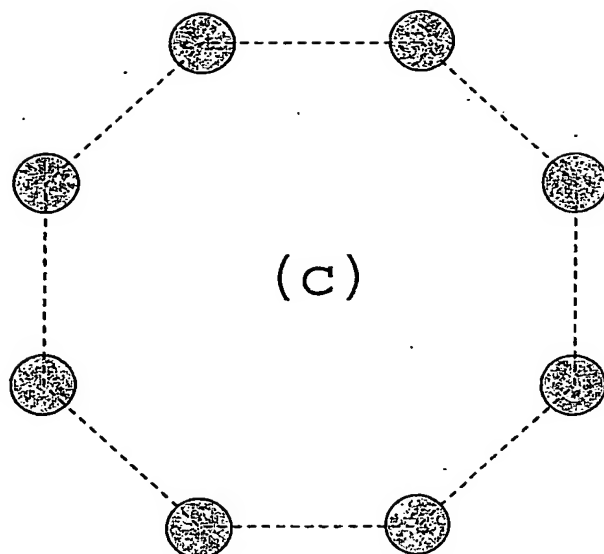
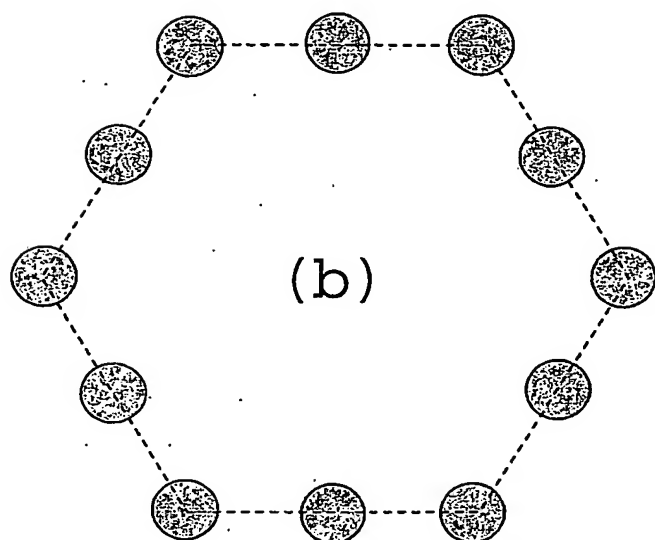
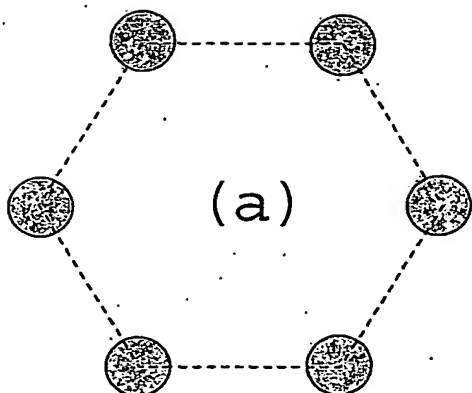
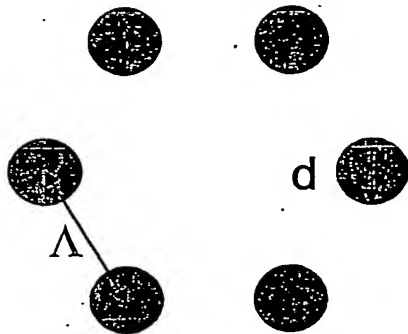
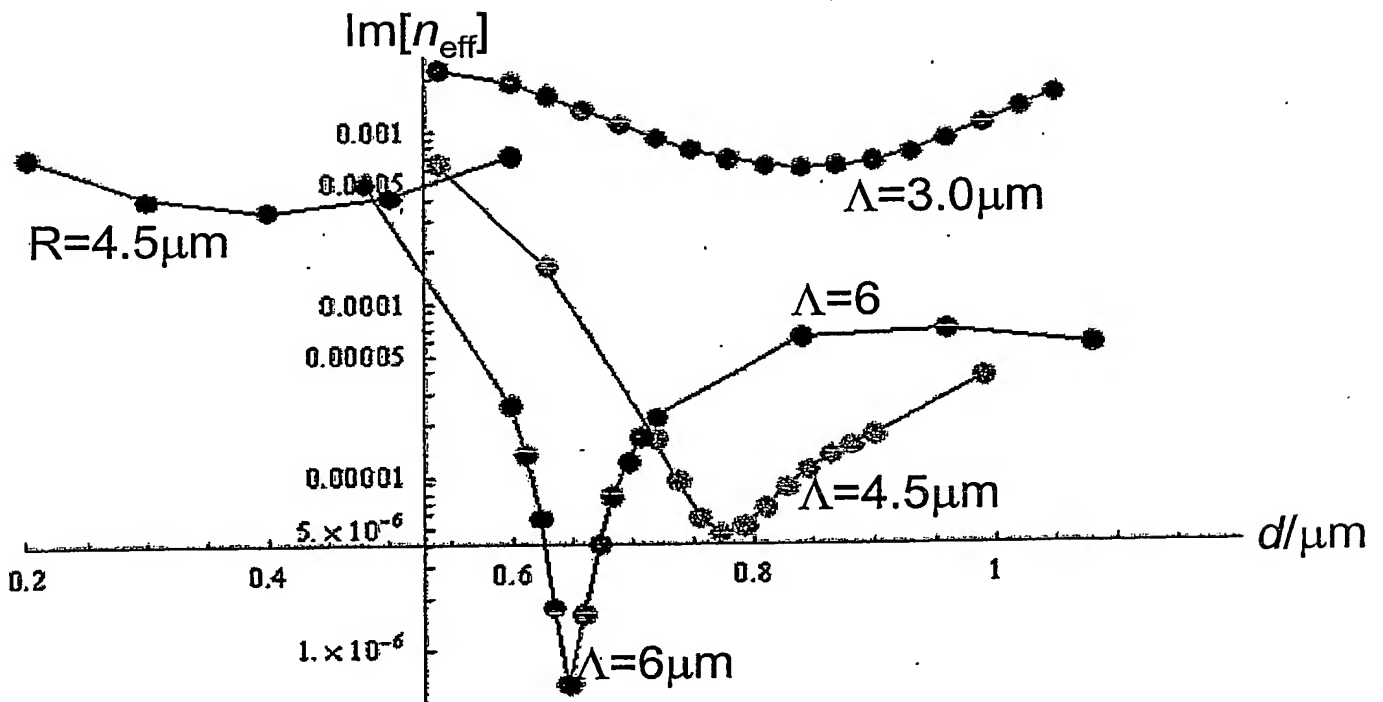
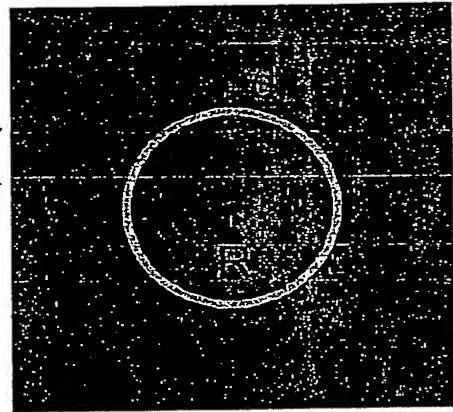


Fig. 16

(a)



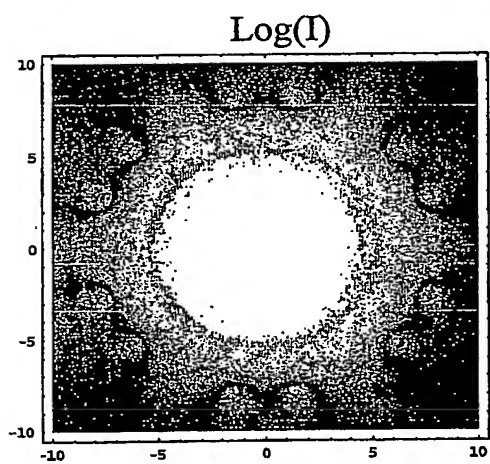
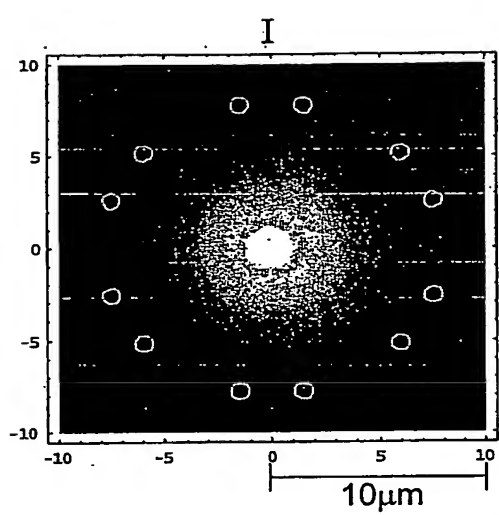
(b)



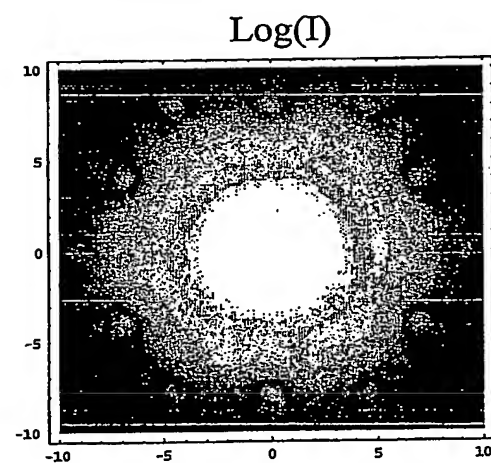
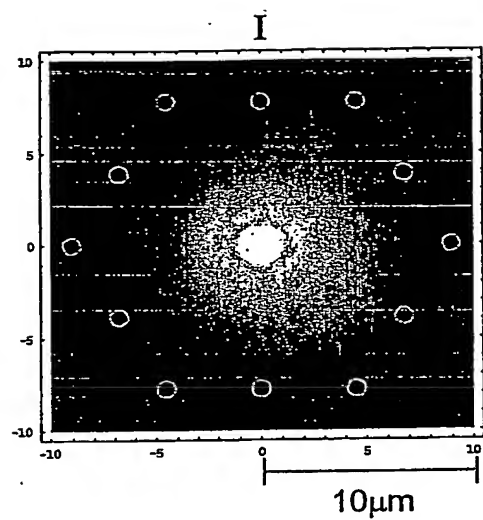
(c)

16/17

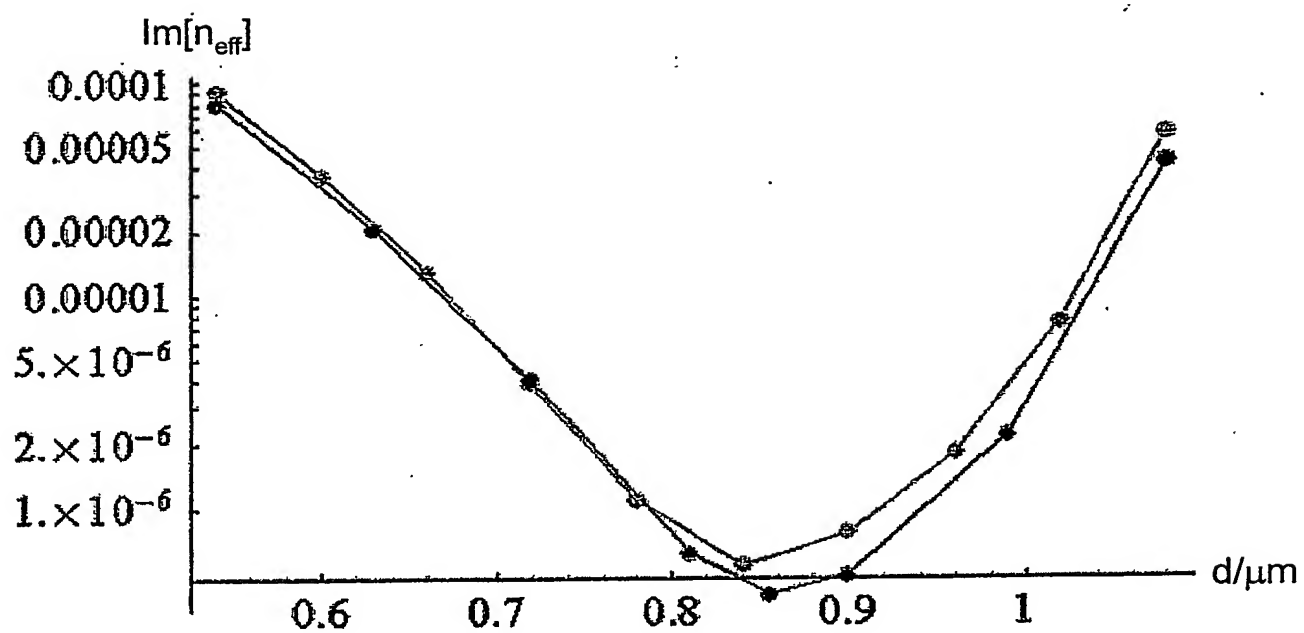
Fig. 17



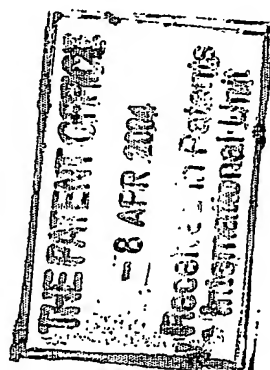
(a)



(b)



PCT/GB2004/001251



This Page is inserted by IFW Indexing and Scanning
Operations and is not part of the Official Record

BEST AVAILABLE IMAGES

Defective images within this document are accurate representations of the original documents submitted by the applicant.

Defects in the images include but are not limited to the items checked:

- ☐ BLACK BORDERS
- ☐ IMAGE CUT OFF AT TOP, BOTTOM OR SIDES
- ☐ FADED TEXT OR DRAWING
- ☒ BLURED OR ILLEGIBLE TEXT OR DRAWING
- ☐ SKEWED/SLANTED IMAGES
- ☐ COLORED OR BLACK AND WHITE PHOTOGRAPHS
- ☐ GRAY SCALE DOCUMENTS
- ☒ LINES OR MARKS ON ORIGINAL DOCUMENT
- ☐ REPERENCE(S) OR EXHIBIT(S) SUBMITTED ARE POOR QUALITY
- ☐ OTHER: _____

IMAGES ARE BEST AVAILABLE COPY.

**As rescanning documents *will not* correct images
problems checked, please do not report the
problems to the IFW Image Problem Mailbox**